Check for updates

ADVANCED MATERIALS
www.advmat.de

2D Materials for All-Solid-State Lithium Batteries

Qianyi Ma, Yun Zheng, Dan Luo, Tyler Or, Yizhou Liu, Leixin Yang, Haozhen Dou, Jiequan Liang, Yihang Nie, Xin Wang, Aiping Yu, and Zhongwei Chen**

Although one of the most mature battery technologies, lithium-ion batteries still have many aspects that have not reached the desired requirements, such as energy density, current density, safety, environmental compatibility, and price. To solve these problems, all-solid-state lithium batteries (ASSLB) based on lithium metal anodes with high energy density and safety have been proposed and become a research hotpot in recent years. Due to the advanced electrochemical properties of 2D materials (2DM), they have been applied to mitigate some of the current problems of ASSLBs, such as high interface impedance and low electrolyte ionic conductivity. In this work, the background and fabrication method of 2DMs are reviewed initially. The improvement strategies of 2DMs are categorized based on their application in the three main components of ASSLBs: The anode, cathode, and electrolyte. Finally, to elucidate the mechanisms of 2DMs in ASSLBs, the role of in situ characterization, synchrotron X-ray techniques, and other advanced characterization are discussed.

1. Introduction

The lithium battery is one of the most important energy storage technologies, which has been widely studied and applied in electric vehicles (EVs), portable electronic devices, and other energy storage products due to their unique advantages including light weight, high specific energy density, and long cycle life.[1–3] However, further development of traditional liquid electrolyte-based lithium batteries is limited due to some shortcomings. The typical organic electrolyte material used in current commercial lithium batteries is flammable and prone to explosion.[4,5] Once a lithium battery generates heat due to long-term operation or damage to its internal structure, organic electrolysis can lead to combustion and explosion.[6] Besides, due to the characteristics of the electrolyte liquid state, the growth of lithium dendrites is likely to occur, resulting in the explosion of lithium batteries due to short circuits.[7–9] Moreover, the electrolyte solution can generate side reactions and affect the reversible capacity and stability of the battery.[10]

In order to relieve or even completely solve these problems, solid state electrolytes (SSEs) without any liquid composition in the electrolyte have been proposed and implemented in lithium batteries, which are called all-solid-state lithium batteries (ASSLBs).[11] Compared with the liquid electrolyte based batteries, ASSLBs have some unique advantages, including inherently nonflammable, sufficient mechanical strength to well suppress lithium dendrites, and good chemical stability to effectively reduce side reactions.[12–14] Besides, the long-term electrochemical and thermal stabilities, as well as the energy density can be further improved by using lithium metal anode in an ASSLB system.[15] Nevertheless, despite the merits of solid-state batteries, there are still some challenges or some key points need to be considered to widely extend the practical application of ASSLBs.[16–19]

To be specific, with the application of the lithium metal anode, the side reactions between the SSEs and lithium metal anode cannot be ignored, which will result in failure of the lithium anode. Moreover, lithium dendrite protrusions from the anode can cause a short circuit thus should be suppressed. Moreover, the high interface resistance between the anode and SSE should be addressed.[20–23] In the cathode side, the low lithium ionic conductivity, poor electronic conductivity, and high interface resistance between electrolyte and cathode and will limit the specific capacity of active materials during charge and discharge process. Second, the volume change of active materials during operation process will reduce the solid–solid interface contract.[24–26]

In the electrolyte, low ionic conductivity in SSEs is one of the limitations of ASSLBs especially for polymer-based SSEs such as polyethylene oxide (PEO). Meanwhile the mechanical strength of SSEs is one of the key parameters to suppress the growth of lithium dendrites.[27–29] The last serious problem is the mechanical stability of the entire solid-state lithium battery.

Q. Ma, Y. Zheng, D. Luo, T. Or, H. Dou, A. Yu, Z. Chen
Department of Chemical Engineering
Waterloo Institute for Nanotechnology
University of Waterloo
Waterloo ON N2L 3G1, Canada
E-mail: zhwchen@uwaterloo.ca
D. Luo, Y. Liu, L. Yang, J. Liang, X. Wang
School of Information and Optoelectronic Science and Engineering
South China Normal University
Guangdong 510006, China
E-mail: wangxin@scnu.edu.cn
Y. Nie, X. Wang
South China Academy of Advanced Optoelectronics & International Academy of Optoelectronics at Zhaoqing
South China Normal University
Guangdong 510006, China
The ORCID identification number(s) for the author(s) of this article can be found under https://doi.org/10.1002/adma.202108079.

DOI: 10.1002/adma.202108079

 © 2022 Wiley-VCH GmbH

During the charging and discharging process, the cathode and anode material of the lithium battery's volume will change. Because it is a solid material, it produces irreversible deformation, resulting in poor contact between the electrode and the electrolyte.[30–33]

To solve the above-mentioned issues and further improve the electrochemical performance of ASSLBs, various advanced materials and structures have been developed in recent years. Among those advanced materials, 2D materials (2DMs) comprised of a single layer of atoms have become a prominent research topic due to their outstanding electrical, electrochemical, thermal, and mechanical properties.[34–36]

To be specific, in the anode side, due to the high chemical stability of 2DMs, 2DMs are applied to alleviate side reactions between the lithium metal anode and electrolyte. In order to deal with the poor interface contract between the anode and electrolyte, 2DMs with high lithium ionic conductivity can be used to form a solid electrolyte interface to reduce the interface resistance and suppress the growth of lithium dendrites.[37,38] In the cathode side, the high specific surface area of 2DMs will enhance the cathode active material loading mass and energy density of ASSLBs.[39] The defect engineering in 2DMs will provide various catalytic active site for active material transformation during charging/discharging process, which is especially necessary for all-solid-state Li–S battery solid phase catalysis.[40] The remarkable electron conductivity of 2DMs can enhance the poor electron conductivity of some active materials to fully utilize the theoretical capacity.[41,42] As for the electrolyte, the high mechanical properties of 2DMs will enhance the mechanical strength of SSEs, especially polymer-based SSEs to suppress the growth of lithium dendrites and extend the cycle life of ASSLBs. Due unique properties of 2DMs, it will provide or enhance the lithium ionic conductivity of SSEs. On the one hand, high specific surface area can provide extra lithium ionic conductivity channel to enhance the lithium transport. On the other hand, for the polymer-based electrolyte, the addition of the 2DMs can reduce the crystallinity of the polymer electrolyte itself to reduce the grain boundary resistance to promote lithium ion transport.[43–45]

Since the discovery of graphene in 2004, various 2DMs have been developed and applied to lithium battery technology, used in electrode materials and electrolytes. In recent years, 2DMs have been continuously applied to ASSLBs and gradually become a research hotspot, however, to the best of our knowledge, there is still no comprehensive summary for 2DMs in ASSLBs. As shown in **Figure 1**, the fundamentals of 2DMs used in ASSLBs including the material classification and synthetic strategies will be first discussed in detail.[46] Then, the latest research progress of 2DMs in material design of ASSLBs will be reviewed systematically, which involves the electrodes, electrolyte, and their interfacial regions. Additionally, a few emerging advanced characterization technologies will be discussed that deepen the understanding of the structure-function relationship in 2DMs for ASSLBs.[47–49] Finally, future research directions are proposed to accelerate the technology developments, from the fundamental understanding of mechanisms to the improvement of materials and applications.

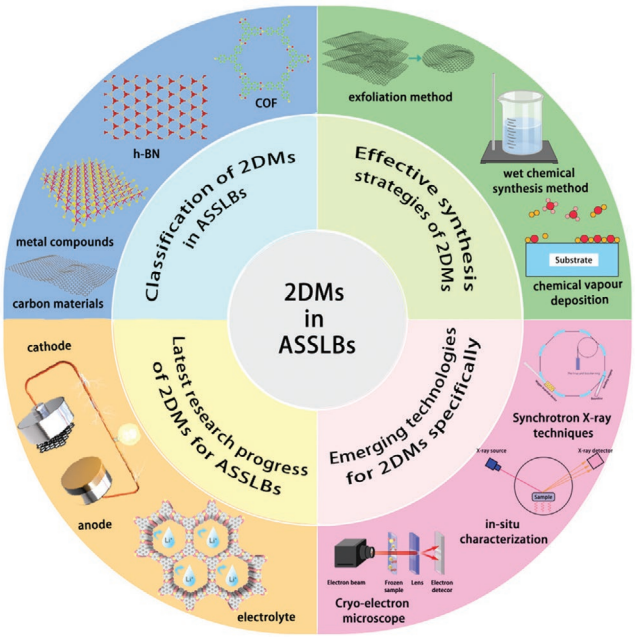

Figure 1. The application of 2DMs in ASSLBs.

2. Fundamentals of 2DMs for ASSLBs

2.1. Classification of 2DMs Used in ASSLBs

Different element compositions will have different effects on the properties and structure of 2DMs. Accordingly, 2DMs are divided into the following categories: carbon-based materials, metallic material, and other 2DMs (**Figure 2**). In this section, the characteristics, and properties of different kinds of 2DMs will be explained.

2.1.1. Carbon Materials

2D carbon materials especially graphene, GO, rGO, et al. have attracted significant interest due to their large specific surface area, low cost, rich resource, high electrical conductivity, and great biocompatibility. These new carbon materials have many excellent physical and chemical properties and are widely used in many fields, especially in the electrochemical field showing their unique advantages.[59] Especially for the application of electrode materials, 2D carbon materials have more unique applications. For specific, the large surface area, and high electrical conductivity can enhance the uniform electron distribution in the electrode structure. Low cost and rich resource can extend the field of the usage of the 2DMs. Biocompatibility can deal with the high interface resistant between electrolyte and electrode.

Graphene was the first discovered and developed 2DM, which is a single layer of graphite comprised of sp^2-hybridized carbon atoms arranged in a hexagonal lattice.[60–62] Based on its special structure, graphene has desirable electrochemical properties like high electrical conductivity, high specific surface area, broad electrochemical window, and high reversible Li storage

© 2022 Wiley-VCH GmbH

15214095, 2022, 16, Downloaded from https://onlinelibrary.wiley.com/doi/10.1002/adma.202108079 by Xian Jiaotong University, Wiley Online Library on [06/06/2024]. See the Terms and Conditions (https://onlinelibrary.wiley.com/terms-and-conditions) on Wiley Online Library for rules of use; OA articles are governed by the applicable Creative Commons License

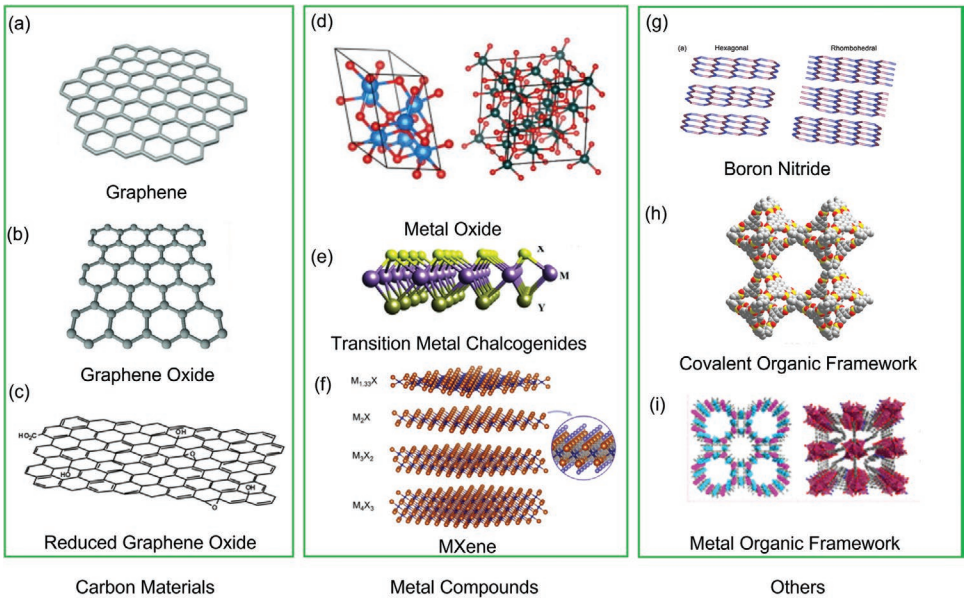

Figure 2. Classification of 2DMs in ASSLBs a) graphene. Reproduced by permission.[50] Copyright 2012, Wiley-VCH. b) graphene oxide. Reproduced by permission.[51] Copyright 1998, American Chemical Society. c) reduced graphene oxide. Reproduced by permission.[52] Copyright 2011, Royal Society of Chemistry. d) metal oxide. Reproduced by permission.[53] Copyright 2021, Elsevier. e) Transition metal chalcogenides. Reproduced by permission.[54] Copyright 2018, Wiley-VCH. f) MXene. Reproduced by permission.[55] Copyright 2020, Elsevier. g) Boron nitride. Reproduced by permission.[56] Copyright 2014, Royal Society of Chemistry. h) Covalent organic framework. Reproduced by permission.[57] Copyright 2015, American Chemical Society. i) Metal organic framework. Reproduced by permission.[58] Copyright 2020, American Chemical Society.

capacity.[63] In ASSLBs, graphene is used as an artificial solid electrolyte interface (SEI) or cathode-electrolyte interface (CEI) for greater interface contract, and as a conductive material for the anode and cathode.[64] Graphene oxide (GO) and reduced graphene oxide (rGO) are the relevant materials for graphene, which has similar properties. In ASSLBs, it is applied to provide extra electronic and ionic transport channel, and deal with the interface problem as CEI.[65–67]

2.1.2. Metal Compounds

Metal compounds are a major portion of inorganic materials applied in ASSLBs that can be divided into three main parts. Metal oxides are often used as cathode materials with high specific capacity and are widely studied. Therefore, the research of metal oxides in the electrochemistry has always been one of the major directions. For 2D metal oxides, such as MnO_2, Co_3O_4, V_2O_5, Li_xMnO_4, each atom within a layer is connected by covalent bonds, while each layer is connected by van der Waals forces.[68] The composition of each layer is metal-oxygen clusters and by sharing corners, edges, and few faces to carry out expansion structure assembly.[69] The covalent bonds and atomic thickness provide the 2D metal oxides some unique properties such as excellent mechanical strength, high active surface, optical transparency, and flexibility.[70,71] Moreover, when 2D metal oxides are arranged in 3D structure, 2D metal oxides strengthen the materials' ability to contain large ions like Li^+.[72,73] In the cathode, metal oxides are used as active material to provide high theoretical capacity and greater interface contract. In the electrolyte, they provide higher mechanical strength and ionic conductivity as the one of the electrolyte components.

With the development of the Li–S battery, research in transition metal chalcogenides (TMCs) has gradually become one of the hotpots, as a result, TMC has been studied and applied in ASSLBs. TMCs such as MoS_2, FeS, TiS_2, Fe_3S_4, VS_2, VS, are a chemical species obtained by the combination of chalcogenide anions with metals.[74] Due to its tunable stoichiometric compositions, unique crystal, rich redox sites, and high electrical conductivity, TMCs attract interest as potential materials for energy storage devices and electrode materials.[75,76] Because of the more lithium insertion/deinsertion site with the high specific surface area, TMCs have higher theoretical special capacity compared with graphite.[77,78] In addition, 2D TMCs are used as the active material in cathode to provide high theory capacity, suppress the side reaction between electrode and electrolyte (especially sulfide-based and oxide-based electrolyte), reduce the percent of crystal region and provide extra lithium transport channel to enhance ionic conductivity. Moreover, when TMCs are used in sulfur-cathode ASSLBs, the "shuttle effect" will be suppressed because the nanostructured TMCs as a polar host can provide stronger affinity with soluble polysulfides, which is because of the polar sulfiphilic surface of TMCs, so that ASSLBs have higher sulfur utilization rate and long cycle life.[79,80]

MXene is one of the newer kinds of 2D transition metal carbides/nitrides. Due to their terminal groups, MXenes are hydrophilic, which is different from most 2DMs. For ASSLBs, with the application of MXene, the terminal group can enhance the interaction between polymer chains and MXene to improve the ionic conductivity of electrolyte.[69]

© 2022 Wiley-VCH GmbH

15214095, 2022, 16, Downloaded from https://onlinelibrary.wiley.com/doi/10.1002/adma.202108079 by Xian Jiaotong University, Wiley Online Library on [06/06/2024]. See the Terms and Conditions (https://onlinelibrary.wiley.com/terms-and-conditions) on Wiley Online Library for rules of use; OA articles are governed by the applicable Creative Commons License

15214095, 2022, 16, Downloaded from https://onlinelibrary.wiley.com/doi/10.1002/adma.202108079 by Xian Jiaotong University, Wiley Online Library on [06/06/2024]. See the Terms and Conditions (https://onlinelibrary.wiley.com/terms-and-conditions) on Wiley Online Library for rules of use; OA articles are governed by the applicable Creative Commons License

2.1.3. Other 2DMs

h-boron nitride (BN), one of the forms of BN, is a 2D material with the same structure as graphene, where the carbon position in the graphene is alternatingly replaced by an equal number of B and N atoms.[81,82] In recent work, h-BN is widely focused on due to its unique properties. First, compared with the graphene, h-BN shows excellent stability in high temperature without the decrease of the layer thick.[83] Second, due to the perfect single atomic layer structure of h-BN, it has excellent high mechanical strength to suppress the growth of the lithium dendrites.[84] Third, h-BN has larger thermal conductivity compared with the bulk h-BN, because when the thickness of the material is scaled down, the phonon–phonon scattering decreases.[85] Moreover, it has chemical inertness, which can help keep it stable against chemicals like Li metal and oxygen.[84,86] Based on its unique properties for SEs, h-BN is used as an additive in PEO to provide extra lithium-ionic transport channels, reduce the crystallinity, and enhance mechanical strength. It also used to suppress side reactions, improving the interfacial contact between the electrode and electrolyte.[87–89]

As the core of energy materials, porous materials are under constant development, where covalent organic framework (COF) has been designed as one of the new porous materials. 2D COF is one kind of porous polymer nanosheets which have highly crystalline structures, tunable function, and high charge-carrier transfer ability.[90] 2D sheets are held together by covalent bonds that constitute the structure of 2D COFs, which are stacked together by noncovalent forces.[91–93] By regulating the types of functional groups, COFs are used individually or as one of the part of electrolyte to transport lithium ions in ASSLBs.[94]

Similar with COFs, as a new generation of materials, 2D MOFs are receiving increasing attention due to their high surface area, structural diversity and high adsorption site density.[95] The metal sites and organic linking groups in MOFs have high chemical bonding and high activity with LiPSs.[96] Through the metal–ligand coordination covalent bond, the active organic substance can be immobilized.[97] In fact, many MOFs can significantly increase the battery capacity retention capacity of lithium batteries. The ion and electron transport in the framework are significantly improved due to application of the porous structure and electrical conductivity of MOFs in solid electrolytes.[98,99]

2.2. Effective Synthesis Strategies of 2DMs

The discovery of graphene immediately made the research of 2DMs the center of materials research. The research on 2DMs with excellent electrochemical properties has gradually become a potential material for the next generation of high-performance ASSLBs.[100] The approaches to prepare various 2DMs can be divided into three parts: 1) exfoliation method 2) chemical vapor deposition 3) wet chemical synthesis method.[34,101]

2.2.1. Exfoliation Methods

Exfoliation method is one of the major methods to fabricate the 2DMs. The mechanism of exfoliation method is to weaken the interaction between nanosheets' layers. Based on the mechanism, the exfoliation can be divided into some parts, such as interaction-assisted expansion and exfoliation, mechanical force-assisted exfoliation, and exfoliation of layered materials containing ions or molecules between the layers, etc.[102,103]

Intercalation-assisted expansion is one of the methods to weaken the interaction between layers using various intercalation agents (**Figure 3**a). Oxidation-based intercalation and reduction-based intercalation method are two major methods to achieve intercalation. Oxidation-based intercalation and exfoliation method involves using strong oxidative agents to intercalate the host gallery of layered materials, which can expand the interlayer spacing of the material to prepare 2DMs such as GO, graphene, h-BN, etc. The main exfoliation conditions can be divided into two kinds with different advantages. One is that by the usage of normal oxidation agents, such as $KMnO_4$, KNO_3, and concentrated H_2SO_4, where production in this condition will be scalable and rich with functional groups. Another one is in the gas phase intercalation using other oxidation agents such as halogen intercalants, metal halides, halides, and super strong oxidizers. The production in this condition will well preserve the in-plate structure and control the intercalation stage. Reduction-based intercalation and exfoliation method involves the assistance of reduction reactions to prepare 2DMs, such as metal chalcogenides, graphene, h-BN. The main exfoliation conditions can be divided into four types and each one has its own advantages.[104] First, the fabrication process in the vacuum condition by gas intercalation of pure alkali metals can prepare TMCs with good conductivity and high percentage of metallic phase with high monolayer yield. Second, the fabrication process is in the liquid phase condition such as n-BuLi, hexane solution, or naphthalide, which can produce TMCs with tunable percentage of metallic phase, semiconductivity, and high monolayer yield. Third, 2DMs can be fabricated by electrochemical intercalation of lithium ions. Reduction-based intercalation and exfoliation based on this condition is safe and suitable for most 2DMs fabrication process. Fourth, in polar aprotic organic solvents conditions, alkali metal atoms are applied to weaken the interaction between layers to produce 2DMs, which is widely applicable for most 2DMs, and easy for assembly without the help of external forces.[105,106]

Mechanical force-assisted exfoliation is one of the fabrication methods to produce 2DMs, which uses external forces to break the internal interaction force between layers. It can be divided into several approaches, such as sonication assisted-exfoliation and shear force-assisted liquid phase exfoliation (Figure 3b), ball milling-assisted exfoliation (Figure 3c), ion exchange-assisted exfoliation, etching and intercalation-assisted exfoliation, etc. The mechanism of sonication assisted-exfoliation and shear force-assisted liquid phase exfoliation is to match the surface energy between the layers to separate it, higher energy to increase the yield and produce 2DMs with well persevered structure and scalable size, such as graphene, h-BN, MoS_2, metal oxide, MOFs, etc. To prepare large quantities 2DMs, ball milling is used to exfoliate layer materials, in which the mechanism is based on a shear force parallel to the layers to weaken the interaction between layered materials. It is also used to produce scalable materials with low cost and large quantities, such as graphene, h-BN, MoS_2.[107,108]

© 2022 Wiley-VCH GmbH

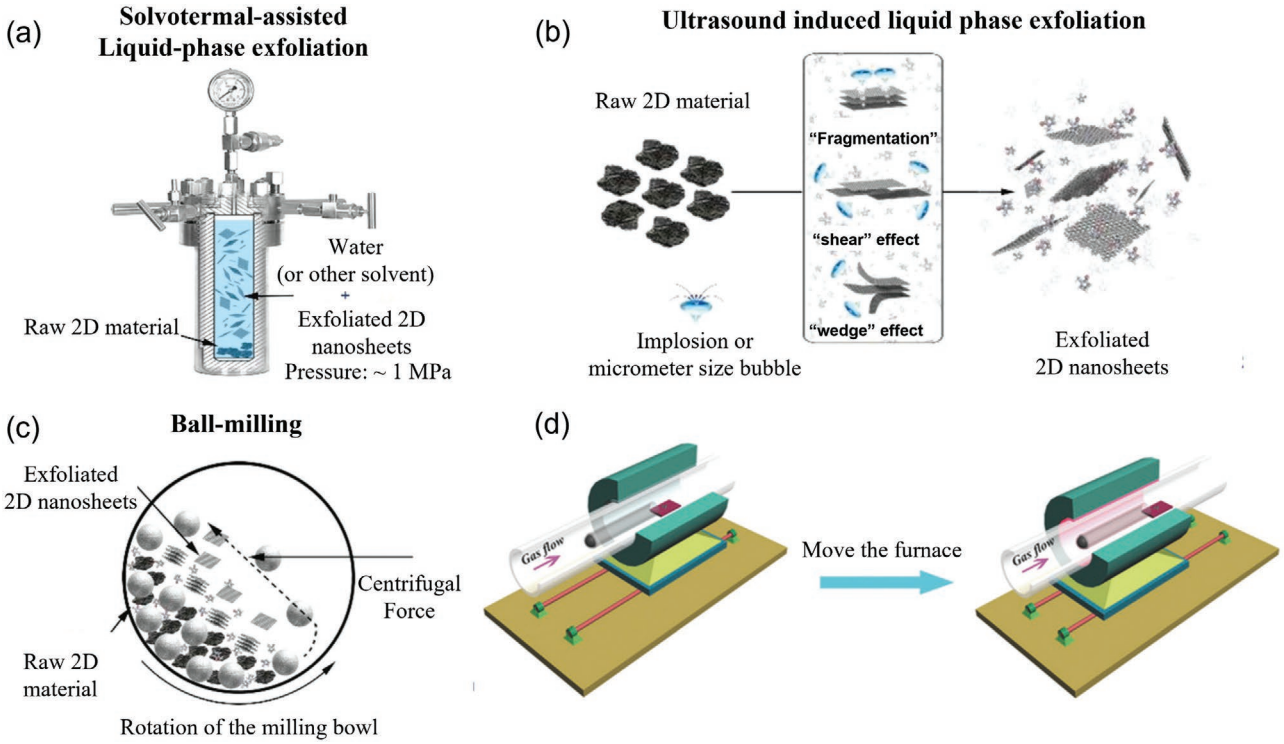

Figure 3. a) Solvothermal-assisted liquid-phase exfoliation; b) ultrasound induced liquid-phase exfoliation; c) ball-milling. Reproduced by permission.[119] Copyright 2019, Wiley-VCH. d) Chemical vapor deposition for 2DMs. Reproduced by permission.[120] Copyright 2018, Wiley-VCH.

With the assistant of ions and molecules to weaken the interlayer interaction between materials, some special 2DMs can be prepared. It can be divided into two parts, one is ion exchange-assisted exfoliation, another one is etching and intercalation-assisted exfoliation. To deal with produce 2DMs that are difficult to exfoliate by the application of oxidation or reduction agents, ion exchange-induced intercalation is applied. To mute the electronic interaction between layers with protons, anionic ions is exchanged with proton to produce 2DMs which are monolayers, with high yield and intrinsically charged sheets, such as layered double hydroxides (LDH). Based on the similar mechanism, the 2DMs which has strong bond between layers such as MXene should be prepared by etching with HF or other organic bases. The production of this method is water soluble and this method is suitable to many materials.[109,110]

2.2.2. Chemical Vapor Deposition

Chemical vapor deposition (CVD) is a technology with a long history and one of the most common technologies to produce 2DMs, which is traditionally used for the preparation of high-quality thin films, such as W, Ti, Ta, Zr, and Si on substrates (Figure 3d).[111] Here, the researchers use CVD to produce single crystal graphene as an example to briefly introduce this technology. The key point in this regard is the need to anneal under relatively high temperature hydrogen, so that the grains are quickly deposited on the substrate and inhibit normal CVD growth. The specific production conditions are hydrogen, methane, and argon as gas conditions, copper foil as a substrate and catalyst, and hydrogen as a cocatalyst, and then single crystal graphene is produced by the CVD process.[112–115] In recent years, 2DMs such as silicene, borophenes, h-BN nanosheets, are always produced by CVD. In addition, compared with other methods, CVD method can fabricate 2D heterostructures. CVD procedures have been used to fabricate both vertical and lateral heterostructures.[116] Vertical heterostructures are mainly synthesized by the following techniques: 2D crystal growth, vapor-solid reactions, and van der Waals epitaxy. Based on its controllable thickness of 2DMs, some micro-ASSLBs have been fabricated by this method.[117,118]

2.2.3. Wet Chemical Synthesis Method

Wet chemical synthesis is a low-cost method that can effectively synthesize several types of carbonaceous and noncarbonaceous 2DMs. The chemical synthesis process is a bottom-up approach in which atoms/molecules are deposited on the substrate and a 2D layered structure is formed through a step-by-step deposition process. Although solvent stripping has been well optimized and is commonly used to synthesize 2D nanostructures, chemical synthesis methods are still under active investigation for further optimization. Basically, these are wet chemistry methods, which react chemically and deposit onto substrates to produce 2D nanostructures.[34,106]

© 2022 Wiley-VCH GmbH

15214095, 2022, 16, Downloaded from https://onlinelibrary.wiley.com/doi/10.1002/adma.202108079 by Xian Jiaotong University, Wiley Online Library on [06/06/2024]. See the Terms and Conditions (https://onlinelibrary.wiley.com/terms-and-conditions) on Wiley Online Library for rules of use; OA articles are governed by the applicable Creative Commons License

3. Research Progress of 2DMs Used in ASSLBs

3.1. 2DMs in Electrodes Design for ASSLBs

In order to meet the performance requirements of materials used in ASSLBs, 2DMs have been introduced into various components of ASSLBs, which includes electrodes, electrolyte, and their interfacial regions. The latest research progress of 2DMs in electrode design of ASSLBs is summarized systematically in this section.

3.1.1. Anode

The anode is one of the key compositions of ASSLBs. Compared with conventional Li ion batteries, requirement of the anode in ASSLBs is higher and more complex. Beside excellent porosity, great chemical stability with electrolytes, light weight, good durability, low cost, voltage match with preferred cathode, good conductivity, high theoretical capacity, and high irreversible capacity, the interface resistance between anode and different type of electrolytes also needs to be considered. Since lithium metal itself has high activity, it will inevitably produce side reactions with the electrolyte, which will increase the interface resistance. In addition, suppressing the growth of lithium dendrites is another serious problem. For Li metal batteries, the uniform deposition of lithium not only improve the coulombic efficiency but also deal with interface contract problem.[121] In this article, the method to develop the anode is to modify the surface of anode or composite electrode by using 2DMs.

Graphene: Graphene is a promising electrode material in lithium-ion batteries due to its high conductivity (≈10^6 S cm^{-1}), high specific surface area (≈2630 m^2 g^{-1}) and high lithium capacity.[66,122] In general, the research of graphene in ASSLBs anode can be divided into two main categories: 1) Anode active material 2) Current collector. According to its feature and function, graphene can be used as high-performance anode for high energy density ASSLBs due to its stratified structure, low mass, and superior electronic conductivity by methods like magnetron sputtering CVD. In this regard, Lin et al. deigned a micro ASSLBs based on pure graphene anode where the electrolyte is LiPON and the cathode is $LiCoO_2$. A thin graphene anode layer was grown via CVD and subsequently sputtered with the electrolyte and cathode layers to obtain a 600 nm thick ASSLB with high energy density.[123] Wei et al. also use CVD method to grow a monolayer graphene onto the surface of Cu to fabricate ASSLBs, in which its energy and power density reaches 10 W h L^{-1} and 300 W L^{-1}, respectively.[66]

On the other hand, due to its high affinity with lithium metal, graphene can be used to modify the surface of Cu to improve the uniform deposition of lithium metal in the anode and the interfacial contact between the anode and electrolyte. For instance, Huang et al. applied vertical graphene on 3D commercial copper mesh to improve the uniformity of lithium deposition, which is due to the dual 3D structure and defects in the vertical structure (**Figure 4**a). Uniform lithium deposition

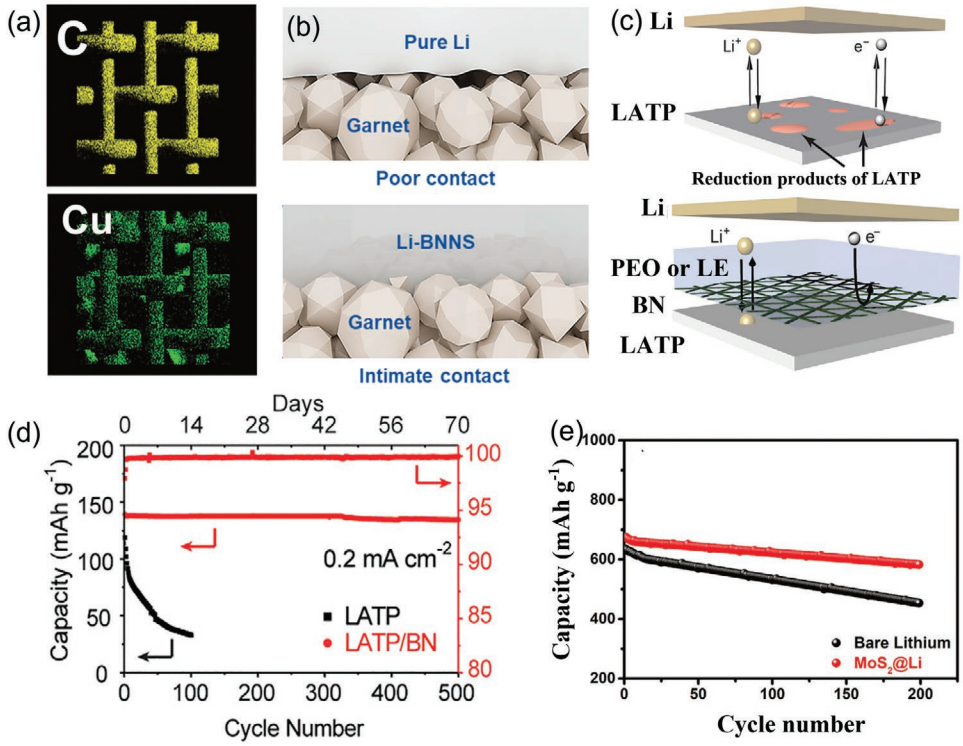

Figure 4. a) 3D Cu/Graphene 3D current collector. Reproduced by permission.[124] Copyright 2019, Wiley-VCH. b) BNNS/Lithium metal composition anode. Reproduced by permission.[125] Copyright 2019, American Chemical Society. c) BN-based anode protection SEI; d) cycling performance of Li|PEO/LATP|LFP cells with and without BN coating. Reproduced by permission.[126] Copyright 2019, Elsevier. e) Cycling performance of Li|MoS_2/$Li_7P_3S_{11}$|S cell. Reproduced by permission.[127] Copyright 2019, Wiley-VCH.

© 2022 Wiley-VCH GmbH

15214095, 2022, 16, Downloaded from https://onlinelibrary.wiley.com/doi/10.1002/adma.202108079 by Xian Jiaotong University, Wiley Online Library on [06/06/2024]. See the Terms and Conditions (https://onlinelibrary.wiley.com/terms-and-conditions) on Wiley Online Library for rules of use; OA articles are governed by the applicable Creative Commons License

and nuclear growth can be verified by X-ray photoelectron spectroscopy (XPS) and energy-dispersive X-ray spectroscopy (EDS) methods. As a result, the assembled ASSLBs with 3D Cu/graphene structure anode shows better cycle stability and lower polarization.[124]

BN: Boron nitride (BN) has similar properties with graphite. It has high chemical and mechanical stability and low electronic conductivity. As a result, the major applications of BN in ASSLBs can be divided into two parts.[125,126] One is to improve the interface contract between the anode and electrolyte due to its high ionic conductivity and low electronic conductivity, where the low electronic conductivity can suppress the growth of lithium. Wen et al. applied 2D boron nitride nanosheets (BNNS) with Li metal to make a composite anode to improve the interface contact between Li metal anode and solid electrolytes (Figure 4b). Only 5 wt% BNNS can significantly improve the mechanical contact between Li metal and garnet-type SSE. As a result, the interfacial resistance is only 9 Ω cm^{-2} which is much lower than without BNNS (560 Ω cm^{-2}). In addition, by using BNNS, the electrochemical plating and striping process is stable for 380 h and shows a high critical current density of 1.5 mA cm^{-2}.[125] Another approach is to use BN as anode protection layer to suppress side reactions between the electrolyte and lithium anode due to its high mechanical and chemical stability. For example, Cheng et al. coated the BN on the anode surface to protect the $Li_{1.3}Al_{0.3}Ti_{1.7}(PO_4)_3$ (LATP) solid electrolyte from reaction with lithium metal by CVD (Figure 4c). In addition, Li|Li symmetrical cell with 1–2 mm of PEO polymer electrolyte at the Li/BN interface shows 500 h of cycle life at 0.3 mA cm^{-2}. The solid-state batteries fabricated with Li|LATP/BN/PEO|$LiFePO_4$ retains 96.6% capacity after 500 cycles (Figure 4d). By the application of in situ transmission electron microscopy (TEM) and cross-sectional scanning electron microscopy (SEM), during the charge and discharge process, there is no structural change with the LATP/BN particle, which indicates no side reaction between the LATP and Li anode.[126]

2D MoS_2: MoS_2 has low electronic conductivity, high ionic conductivity, and high selective ion transport, which is suitable to be used as the protection interface on the surface of lithium anode to prevent the direct contact between the anode and cathode. For example, Kızılaslan et al. applied 2D MoS_2 as the protective interface to replace the bilayer solid electrolyte design in ASSLBs. By the application of MoS_2, the ASSLBs exhibits 675.8 mA h g^{-1} initial capacity and 584.1 mA h g^{-1} final capacity at 0.4 mA cm^{-2}, and after 200 cycles, MoS_2 ASSLBs fade by 13.58%, while ASSLBs without MoS_2 fade 27.3% (Figure 4e).[127,128]

3.1.2. Cathode

The cathode is a key component of ASSLBs and the interfacial contact between the cathode and electrolyte is also an essential challenge in ASSLBs. Ionic diffusion is influenced by the poor interface contract between the electrode and electrolyte. Due to the volume change of active materials during the lithiation and delithiation process, physical degradation occurs which will cause increased interface resistance, heterogeneous ion transport, and poor mechanical contact. In order to deal with these problems, 2DMs are used in ASSLBs.[129]

Graphene Relevant:

(1) Graphene

Due to the excellent electrochemical properties and the layered structure of graphene, it is one of the most promising materials for the cathode of ASSLBs. The major effects of graphene can be divided into three parts.

First, due to the high specific surface area and flexibility of graphene, it is used to modify the surface of cathode to improve the surface contract with solid electrolytes. For instance, Li et al. use electrochemical prelithiation to construct a LiF/graphene inorganic composite interface on the interface between cathode and garnet electrolyte, which is in situ converted from fluorinated graphene (GF) and the cathode materials (**Figure 5**a). Graphene is used to improve the surface mechanical contact between LiF and the garnet electrolyte. The effect of LiF is to enhance the transport of Li-ions in the cathode side due to its high chemical/thermal stability and low surface diffusion. Li|garnet/ICI|$LiFePO_4$ ASSLBs were tested at 0.05 C at 60 °C, which retains 90% capacity after 60 cycles, indicating that the LiF/graphene ino rganic composite interface can improve interface issues between the cathode and garnet.[130]

Second, because graphene has high electronic conductivity, graphene is used to enhance the electronic conductivity, which is similar to the application of graphene in the anode of ASSLBs. Cai et al. used $CuCo_2S_4$/graphene/10%$Li_7P_3S_{11}$ as the cathode for high performance ASSLBs (Figure 5b). $Li_7P_3S_{11}$ is coated to deal with the contact problem between the cathode and electrolyte, while graphene is used to improve the electronic conductivity. The combination of $CuCo_2S_4$ and graphene is to balance the electronic and ionic conductivities. The ASSLBs with composite cathode yields 556.41 mA h g^{-1} reversible capacity at 500 mA g^{-1} after 100 cycles, which shows great cycling stability and high performance.[131] In order to fully present the ability of graphene to construct a 3D ionic and electronic network, Wan et al. designed Cu_2SnS_3/graphene/$Li_7P_3S_{11}$ nanocomposite cathodes, where Cu_2SnS_3 nanoparticles are evenly distributed in graphene nanosheets (Figure 5c). The major effect of graphene is to ensure the high electronic conduction of cathode. The nanoparticles and nanosheets contribute to the high electron and ionic conductivities which enable high energy density in ASSLBs and reduce the volume change to extend the cycle life of ASSLBs. At 100 mA g^{-1}, the ASSLBs with Cu_2SnS_3/graphene/$Li_7P_3S_{11}$ nanocomposite cathodes show high reversible discharge specific capacity of 813.2 mA h g^{-1} and after 60 cycles, it retains 732.0 mA h g^{-1}. At 500 mA g^{-1} after 200 cycles, it retains 363.5 mA h g^{-1}.[132]

Third, aside from being an additive material to enhance the electronic conductivity and surface contact between the cathode and electrolyte, graphene can also be used as a promoter to inhibit material aggregation and improve material contact. For instance, Wan et al. applied graphene into Cu_2ZnSnS_4 (CZTS) to fabricate the composite anode with enhanced electrochemical performance and stability. To be specific, compared with

© 2022 Wiley-VCH GmbH

15214095, 2022, 16, Downloaded from https://onlinelibrary.wiley.com/doi/10.1002/adma.202108079 by Xian Jiaotong University, Wiley Online Library on [06/06/2024]. See the Terms and Conditions (https://onlinelibrary.wiley.com/terms-and-conditions) on Wiley Online Library for rules of use; OA articles are governed by the applicable Creative Commons License

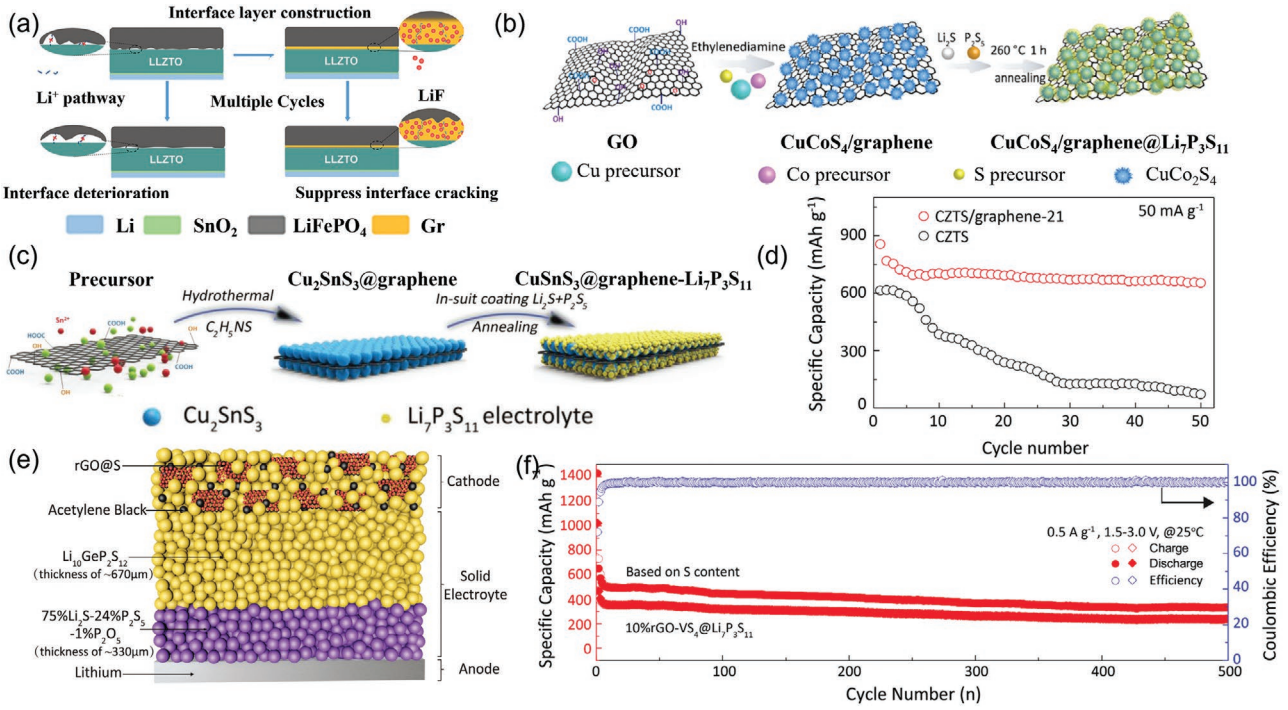

Figure 5. a) LiF/graphene inorganic composite interlayer. Reproduced by permission.[130] Copyright 2020, Royal Society of Chemistry. b) $CuCo_2S_4$/Graphene@$Li_7P_3S_{11}$ nanocomposite. Reproduced by permission.[131] Copyright 2020, American Chemical Society. c) Cu_2SnS_3@graphene-$Li_7P_3S_{11}$ nanocomposite. Reproduced by permission.[132] Copyright 2019, Wiley-VCH. d) Cyclic performances for CZTS and CZTS/graphene-21. Reproduced by permission.[133] Copyright 2016, Elsevier. e) rGO@S-$Li_{10}GeP_2S_{12}$-acetylene black (AB) composite cathode. Reproduced by permission.[137] Copyright 2017, Wiley-VCH. f) 10%rGO-VS_4@$Li_7P_3S_{11}$ cathodes between 1.5 and 3.0 V at 0.5 A g^{-1}. Reproduced by permission.[140] Copyright 2019, Elsevier.

pure CZTS, the addition of graphene can provide electronic conductivity pathways, mitigate anode active material degradation caused by the volume changes, inhibit the aggregation of active materials, and improve the contract between the electrolyte and active materials. As a result, good electrochemical performance has been achieved, the capacity of the CZTS/graphene is 760.4 mA h g^{-1}, which is higher than that of pure CZTS (632.3 mA h g^{-1}), and the ASSLB shows a discharge capacity of 645.4 mA h g^{-1} after 50 cycles and an energy density of 346.2 W h kg^{-1} (Figure 5d).[133]

(2) GO

GO is the oxidized derivative of graphene. It has similar structure with graphene which can provide extra ionic channel. As a result, it has potential to be used in the ASSLBs. The major application of GO can be divided into two parts.

Due to its layered structure, the GO provides extra ionic transport channels. Zhang et al. designed a carbon matrix (GO-PEG) with lithium-ion conductor (PEG) as the cathode to load sulfur for all-solid-state lithium–sulfur batteries. The surface of the GO-PEG contains evenly distributed sulfide GO–PEG@C/S cathode through a one-pot reaction. In addition, by the application of GO, it enables the uniform distribution of super P to improve the electronic conductivity. At 0.2 C and 80 °C, the ASSLBs with GO–PEG@C/S cathode shows an initial capacity of 1225 mA h g^{-1}. At 2C and 80 °C, this ASSLB retains 86.6% capacity after 100 cycles.[134]

On the other hand, GO has high ionic conductivity to be used at the surface interface, which will not influence the electrochemical performance of ASSLBs. GO can prevent the direct contact between cathode and electrolyte to suppress side reactions. For example, Zhuang et al. applied graphene oxide at the interface to suppress side reactions. They studied the reaction between the cathode-$LiNi_{0.5}Co_{0.2}Mn_{0.3}O_2$ and polymer electrolyte-PPE, where the oxidized products Ni^{3+} and Co^{4+} will cause the decomposition of PPE. In order to avoid the side reaction, graphene oxide was used to coat the $LiNi_{0.5}Co_{0.2}Mn_{0.3}O_2$ cathode, as a result, the ASSLB shows higher initial capacity, cycle life and interface contract. After 300 cycles, it retains 69.2% capacity at 0.3 C.[135]

(3) rGO

rGO has a structure that is highly similar to graphene, therefore it has similar properties to graphene, with high electronic conductivity, large surface area, excellent mechanical strength, and excellent flexibility. High surface area, excellent flexibility, and great mechanical strength can buffer the volume changes in the cathode, which can significantly improve the interfacial contact and cycle life of the ASSLBs. As a result, The main effects of rGO in the cathode can be divided into two parts.[136]

Based on the similar structure with graphene, rGO can be used to modify the surface of cathode to improve the interfacial contact between the cathode and electrolyte. For instance, Yao et al. coated 2 nm of sulfur on the surface of rGO to reduce

© 2022 Wiley-VCH GmbH

15214095, 2022, 16, Downloaded from https://onlinelibrary.wiley.com/doi/10.1002/adma.202108079 by Xian Jiaotong University, Wiley Online Library on [06/06/2024]. See the Terms and Conditions (https://onlinelibrary.wiley.com/terms-and-conditions) on Wiley Online Library for rules of use; OA articles are governed by the applicable Creative Commons License

15214095, 2022, 16, Downloaded from https://onlinelibrary.wiley.com/doi/10.1002/adma.202108079 by Xian Jiaotong University, Wiley Online Library on [06/06/2024]. See the Terms and Conditions (https://onlinelibrary.wiley.com/terms-and-conditions) on Wiley Online Library for rules of use; OA articles are governed by the applicable Creative Commons License

the interface resistance, strain and stress between the sulfur cathode and SSEs in ASSLBs, where the sulfur is uniformly distributed on the surface of rGO (Figure 5e). Compared with the Li–sulfur battery that utilizes liquid electrolyte, rGO@S-$Li_{10}GeP_2S_{12}$-acetylene black composite cathode shows similar electrochemical performance in ASSLBs. At 0.1, 0.5, 1.0, 2.0, and 5.0 C it respectively achieves 1384.5, 1336.3, 903.2, 502.6, and 204.7 mA h g^{-1} capacity. After 50 cycles at 1.0 C, a capacity of 830 mA h g^{-1} was retained. By the application of rGO, the volume change process during lithiation and delithiation becomes uniforms, which extends the cycle life of ASSLBs because of reduced stress and strain.[137]

In addition, the layered structure of rGO can provide extra electronic and ionic channels to enhance electronic performance. In preliminary work, Yue et al. simply combined rGO with V_2O_5 nanowires to fabricate an rGO composite paper cathode to increase the electronic conductivity of ASSLBs, where uniform distribution of the V_2O_5 nanowires was observed by SEM. PEO-MIL-53(Al)-LiTFSI lithium–vanadium batteries whose cathode is V_2O_5 nanowire–rGO composite paper were produced, which can work at high temperature and has high safety. Under the condition of 17 mA g^{-1}, the average capacity of the lithium battery can reach 329.2 mA h g^{-1}, and the capacity remains stable after 40 cycles. In addition, the lithium ion storge performance is fast and stable at 80 °C with a voltage window of 1.0–4.0 V.[138] To further improve the combination of rGO and active materials, Zhang et al. designed a new 10% rGO-VS_4@$Li_7P_3S_{11}$ nanocomposite as the cathode of ASSLBs, where the VS_4 grows smoothly on the surface of rGO nanosheets. At 0.1 A g^{-1}, Li|75%Li_2S-24%P_2S_5-1%P_2O_5|$Li_{10}GeP_2S_{12}$/10%rGO-VS_4@$Li_7P_3S_{11}$ ASSLBs show a high reversible capacity of 611 mA h g^{-1} after 100 cycles.[139] In addition, in order to systematically evaluate the effect of rGO in cathode, Zhang et al. also applied MoS_3 nanoparticles onto the surface of the rGO as the cathode by the replacement of VS_4. By the application of nanoparticle and 2DMs, the volume change becomes smaller, and electronic conductivity is improved due the addition of 2DMs. At 0.1 A g^{-1}, after 100 cycles, the Li|75%Li_2S–24%P_2S_5–1%P_2O_5|$Li_{10}GeP_2S_{12}$/rGO-MoS_3 ASSLBs show 553.4 mA h g^{-1} reversible capacity. The improvement is more significantly at high currents, at 1.0 A g^{-1}, after 500 cycles, it retains 414.1 mA h g^{-1} (Figure 5f).[140]

2D Transition Metal Chalcogenides (TMC): 2D TMC is another potential material used in ASSLBs. Compared with traditional cathode materials, the application of transition metal sulfides will significantly decrease the interface resistance between cathode and electrolyte. Besides, TMCs can be used as active material to provide the high reversible capacity density and moderate operating voltage of ASSLBs. Moreover, based on its 2D structure, 2D TMCs can provide extra lithium-ion transport compared with bulk transition metal sulfide. The major feature of different TMCs can be divided into three kinds.

Initially, some kinds of 2D TMCs are used to provide high ionic conductivity and great interface compatibility, which is essential to deal with the low conductivity and high resistance problem. Santhosha et al. compared bulk MoS_2 with 2D layered MoS_2 to show the superiority of 2DMs in ASSLBs (**Figure 6**a). 2D MoS_2 is excellent and suitable for ASSLBs, which has 670 mA h g^{-1} theoretical capacity, 1.54 V theoretical redox potential, and 10^{-4} Ω cm^{-1} electronic conductivity. Moreover, 2D MoS_2 has small volume change compared with typical cathode materials, which is essential for ASSLBs to deal with the loss of contact resulting in high resistance.[141,142] In theory, based on the nanostructure of 2D layered MoS_2, MoS_2 will have high specific surface area, which can lower the contact resistance with the electrolyte. 2D layered MoS_2 also enables 2D diffusion because of its 2D structure for the intercalation process of Li. MoS_2 was used to prepare the composite cathode. The cathode uses 3 tons and contain 60 wt% MoS_2, 30 wt% β-Li_3PS_4 solid electrolyte, and 10 wt% carbon blacks by cold-pressing. The SE use β-Li_3PS_4, while the anode uses Li-In alloy. The initial specific capacity is 439 mA h g^{-1} in 67 mA g^{-1} in the 0.01–3.0 V range. After 500 cycles, it retains a battery capacity of 312 mA h g^{-1}. By substituting the 2D layer MoS_2 with bulk MoS_2, the initial discharge capacity is only 259 mA h g^{-1}.[142]

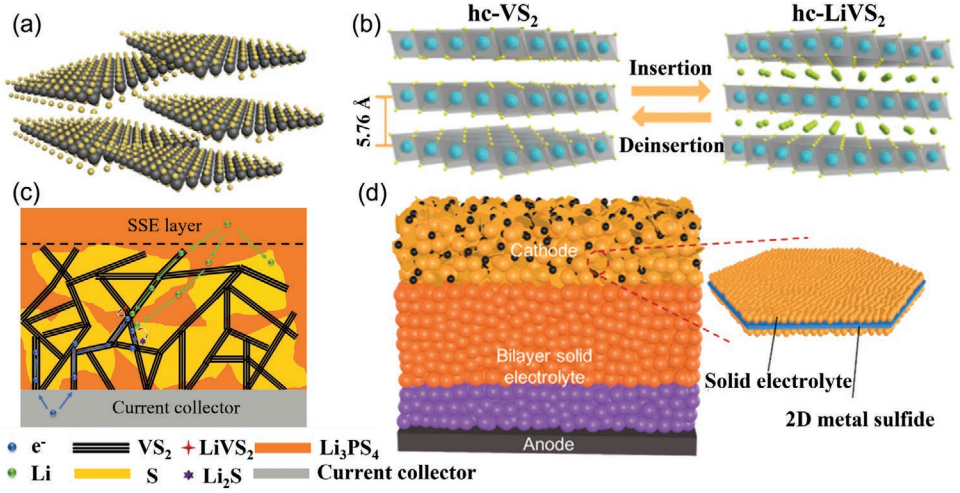

Figure 6. a) Exfoliated MoS_2 nanosheets. Reproduced by permission.[142] Copyright 2019, American Chemical Society. b) Highly crystalline layered VS_2 (hc-VS_2) nanosheets. Reproduced by permission.[146] Copyright 2018, American Chemical Society. c) Proposed microstructure and discharge mechanism for the solid-state hybrid Li-S/VS_2 battery. Reproduced by permission.[148] Copyright 2020, Wiley-VCH. d) Monodispersed 2D Co_3S_4 hexagonal platelets. Reproduced by permission.[150] Copyright 2020, American Chemical Society.

 © 2022 Wiley-VCH GmbH

Other kinds of transition metal sulfide are desirable due to their affordable cost, environmentally benignity, and abundant resources. As the representative transition metal, Fe has been extensively explored. Zhang et al. designed an FeS-based cathode which has high theoretical specific capacity of about 609 mA h g^{-1} and stable reversible capacity.[143] FeS nanoparticles were synthesized by a polyvinyl alcohol precipitation method. Based on SEM observations, the morphology comprised a flower-like structure which is about 300 nm and with some sheet-like subunits. This special structure provides some void space, which can buffer the electrode's volume change in the charge and discharge process that can cause losses of mechanical contract.[144,145] With the application of thin FeS nanosheets, the Li ion pathway will become shorter, and the Li ion insertion and extraction kinetics will be improved. By using nitrogen adsorption–desorption measurements, the specific surface area of FeS nanosheets is 60.31 m^2 g^{-1}. The large specific surface generates more reaction sites for the Li ion insertion and extraction process. The obtained all-solid-state lithium battery displays a reversible discharge capacity of 550 mA h g^{-1} after 50 cycles at 0.1 A g^{-1}. Even if the current density is increased to 1.0 A g^{-1}, the specific discharge capacity is 403 mA h g^{-1}. To improve the interface contact between the electrolyte and cathode, Fe_3S_4 was also explored. As Fe_3S_4 has a combination of +2 and +3 valence of Fe, it shows excellent electrochemical performance compared to FeS. Zhang applied Fe_3S_4 ultrathin nanosheets, which also serves as the cathode active material, onto $Li_7P_3S_{11}$ for ASSLBs by an in-situ approach. The interface contact of Fe_3S_4@$Li_7P_3S_{11}$ nanocomposites is better than pristine Fe_3S_4 nanosheets, which shows 1001 mA h g^{-1}capacity after 200 cycles.[143] Besides Fe, V-based cathode materials such as V_2O_5 have also been applied. As a 2D sulfide, a high-crystallinity VS_2 sheet with a thickness of 50 nm has been used as a new 2DMs to improve the performance of ASSLBs' cathodes (Figure 6b). VS_2 has a hexagonal transition metal hydrogen disulfide structure, so VS_2 has high electronic conductivity and high specific surface area. Cai et al. applied hc-VS_2 as cathode materials, which demonstrates great interface compatibility with P_2S_5 sulfide electrolyte. The experimental results show that under the condition of 50 mA g^{-1}, the high crystallinity VS_2 sheet has high reversibility, and the capacity after 30 cycles is 532.2 mA h g^{-1}.[146,147] After 100 cycles, at 100 and 500 mA g^{-1}, the stable discharge capacity of the all-solid-state lithium battery is maintained at 436.8 and 270.4 mA h g^{-1} respectively.[148]

Furthermore, compared with bulk TMCs, 2D TMCs have high mechanical strength, which not only can used as host material for active material–sulfur, but also can deliver high reversible specific capacity for ASSLBs. Xu et al. designed a new type of intercalation-conversion hybrid cathode with VS_2 nanosheets which was used in ASSLBs (Figure 6c). In this design cathode, on the one hand, VS_2 not only provides electron transport channel like most 2DMs, but also contributes the extra capacity. One the other hand, lithiated VS_2 (Li_xVS_2) can provide extra Li transport channels. The sulfur utilization of Li|Li_3PS_4|S/VS_2/Li_3PS_4 ASSLBs is 85% and the coulombic efficiency is close to 100%. Moreover, the active material loading and an areal capacity of this kind of ASSLB reaches the practical requirement of Li–S batteries, which is 15.5 mg cm^{-2} and 7.8 mA h cm^{-2}, relatively.[148]

Other Types of 2DMs: Other materials include organic, metal oxide, and carbon materials. The major application of these materials can be divided into two parts. One of major application of these kinds of 2DMs is to enhance the ionic conductivity of active materials as the additives. Organic materials are one kind active material which has high theoretical capacity. However, one the main disadvantage of organic cathodes is the low ionic conductivity which limits the performance of the lithium battery. In order to deal with this problem, Fujii et al. applied 2D HHP ($(CH_3(CH_2)_2NH_3)_2$-$(CH_3NH_3)2Pb_3Br_{10}$) in ASSLBs with sulfide solid electrolyte. The recent report shows the mechanism of the insertion and extraction of lithium, which implies the potential of this material applied in the ASSLBs. 2D HHP inherently has Li-ion conductivity, which can reach to about 10^{-3} S cm^{-1}. At 100 °C, the resistance between the electrode and solid electrolyte is only 13 Ω. The ASSLB retains 242 mA h g^{-1} after 30 cycles at 0.13 mA cm^{-2}.[149] Shi et al. applied 2D Co_3S_4 hexagonal nanosheets as cathodes to improve the interface contact and Li-ion conductivity of ASSLBs. 2D Co_3S_4 hexagonal nanosheets were used in a liquid-phase method to coat the surface of $Li_7P_3S_{11}$ (Figure 6d). This structure provides shorter Li-ion transport channels and excellent machine contact due to the large surface area of 2DMs. At 0.5 A, after 50 cycles, the ASSLBs with Co_3S_4@$Li_7P_3S_{11}$ composite cathode exhibits 685.9 mA h g^{-1} reversible capacity. At 1 A, after 100 cycles, it retains 457.3 mA h g^{-1}.[150]

Metal oxides are the conventional cathode material for lithium-ion batteries. In order to improve the ionic conductivity and energy density, Xia et al. designed Li_xMnO_2 nanosheets to fabricate a 3D-structured cathode for ASSLBs. This cathode design showed a high electrochemical tunnel intergrowth structure, which provides alternating 1×3 and 1×2 tunnels. In addition, this 3D structure provides shorter Li-ion transport length, better interface contract, and great mechanical strength. At 50 mA g^{-1}, the Li_xMnO_2/LiPON/Li ASSLB yields 185 mA h g^{-1} and retains 81.3% after 1000 cycles.[151]

Carbon nanosheets are used as the electronic conductive material to improve the interface contact in ASSLBs. V_2O_5 is one of the new lithium-free cathode materials. However, its high-volume change and poor contact with the electrolyte are challenges for implementation in ASSLBs. The nanomodification of V_2O_5 is insufficient to solve these problems. Thus, Su et al. coupled carbon nanosheets with the V_2O_5 cathode. Sub-10 nm V_2O_5/C nanosheets were used as the cathode, which shows excellent contact between the electrode and electrolyte and great interface stability. In addition, by the application of carbon nanostructure, the volume change of V_2O_5 is suppressed, which avoids cracking and pulverization of the surface and improves the electronic conductivity. The ASSLBs with V_2O_5/carbon nanosheet cathode is 228 mA h g^{-1} at 0.1 C and ≈110 mA h g^{-1} at 2.0 C after 50 cycles.[152,153]

3.2. 2DMs in Electrolyte Design of ASSLBs

The electrolyte in ASSLBs mainly includes three types of materials: polymers, oxides and sulfides. Due to different physical, chemical, and electrochemical properties, these three kinds of SEs encounter different problems in ASSLBs. High-performance

© 2022 Wiley-VCH GmbH

15214095, 2022, 16, Downloaded from https://onlinelibrary.wiley.com/doi/10.1002/adma.202108079 by Xian Jiaotong University, Wiley Online Library on [06/06/2024]. See the Terms and Conditions (https://onlinelibrary.wiley.com/terms-and-conditions) on Wiley Online Library for rules of use; OA articles are governed by the applicable Creative Commons License

15214095, 2022, 16, Downloaded from https://onlinelibrary.wiley.com/doi/10.1002/adma.202108079 by Xian Jiaotong University, Wiley Online Library on [06/06/2024]. See the Terms and Conditions (https://onlinelibrary.wiley.com/terms-and-conditions) on Wiley Online Library for rules of use; OA articles are governed by the applicable Creative Commons License

SEs require certain properties, such as high ionic conductivity in room temperature, high thermal stability, great chemical stability, good contract with electron in both physics and chemistry. In this section, we discuss how to use different 2DMs to solve the problems encountered by different solid electrolytes.[154]

3.2.1. Solid Polymer Electrolytes (SPE)

SPEs used in the ASSLBs such as polyethylene oxide (PEO), poly(acrylonitrile) (PAN), poly(vinylidene fluoride) (PVDF), have similar problems in ionic conductivity, low mechanical strength, and limited lithium ionic transport channels. Segmental motion is the main mechanism for the Li ions transport in the polymer-based electrolyte. Compared with the ion conduction in the liquid, this conduction mechanism is more dependent on temperature to reduce the grain boundary resistance of the polymer electrolyte. Therefore, at room temperature, the ionic conductivity of the polymer solid electrolyte is extremely low. In conclusion, high ionic conductivity, high chemical and thermal stability, and great interface contract should be achieved in SPEs. This part will introduce the application of 2DMs to deal with these limitations.[129]

PEO-Based Solid Polymer Electrolytes: PEO is a widely used polymer electrolyte which has high performance. Li ions can move in PEO through chain segmental motions.[126] Based on the mechanism of lithium-ion transport in PEO, the conductivity of Li ion is influenced by the motion of the amorphous phase of PEO. Due to the highly crystalline structure of PEO, the Li-ion conductivity of PEO is only 10^{-6}–10^{-8} S cm^{-1} at room temperature. At higher temperatures, PEO's Li-ion conductivity will be significantly enhanced, although high temperature will reduce the mechanical strength and chemical stability. In order to deal these problems, 2DMs are used to improve the electrochemical performance by its unique structure. The effect of 2DMs in PEO can be divided into three parts.

First, 2DMs can reduce the crystallinity of PEO to enhance the ionic conductivity of PEO. There are two ways to incorporate 2DMs in PEO. One is due to the hydrophilic surface in materials to interact with oxygen through hydrogen bonds with PEO. In the first way, three main kinds of materials are listed here. The first material is MXene, where Pan et al. added hydrophilic $Ti_3C_2T_x$ into PEO_{20}-LiTFSI to reduce the crystallinity of PEO and enhance the ionic conductivity (**Figure 7**a). The PEO with 3.6 wt% MXene shows great ionic conductivity which is 2.2×10^{-5} S m^{-1} at 28 °C. The $LiFePO_4/PEO_{20}$-LiTFSI/Li with 1.5 wt% MXene has been tested in here, it shows stable capacity (140 mA h g^{-1}) at 60 °C after 50 cycles.[155] The second way is using carbon materials. Esfandeh et al. produced SSEs based on polyethylene oxide (PEO) which contains pristine graphene (GnP) or polyethylene glycol grafted graphene (FGnP)[159] The synthesized SSE was characterized using SEM, differential scanning calorimetry (DSC), X-ray diffraction (XRD), and polarization state optical microscope (POM), which verifies that the crystallinity of the nanocomposite electrolyte was reduced.[160] The specific antinucleation effects of GnP and FGnP can be obtained through the image of POM. The specific properties of FGnP can be attributed to the fact that PEO molecules grafted on FGnP can interact with oxygen through hydrogen bonds and limit crystallization.[159] As a result, at room temperature, the ionic conductivity of SPE/FGnP (0.5%) is significantly improved (2.53×10^{-5} S cm^{-1}), and the mechanical stability is also improved.[159] The third material is MOF. Han et al. incorporated nickel-based ultrathin metal–organic framework (MOF) nanosheets (NMS) into PEO. Due to the high aspect ratio of NMS, the application of NMS significantly reduces the

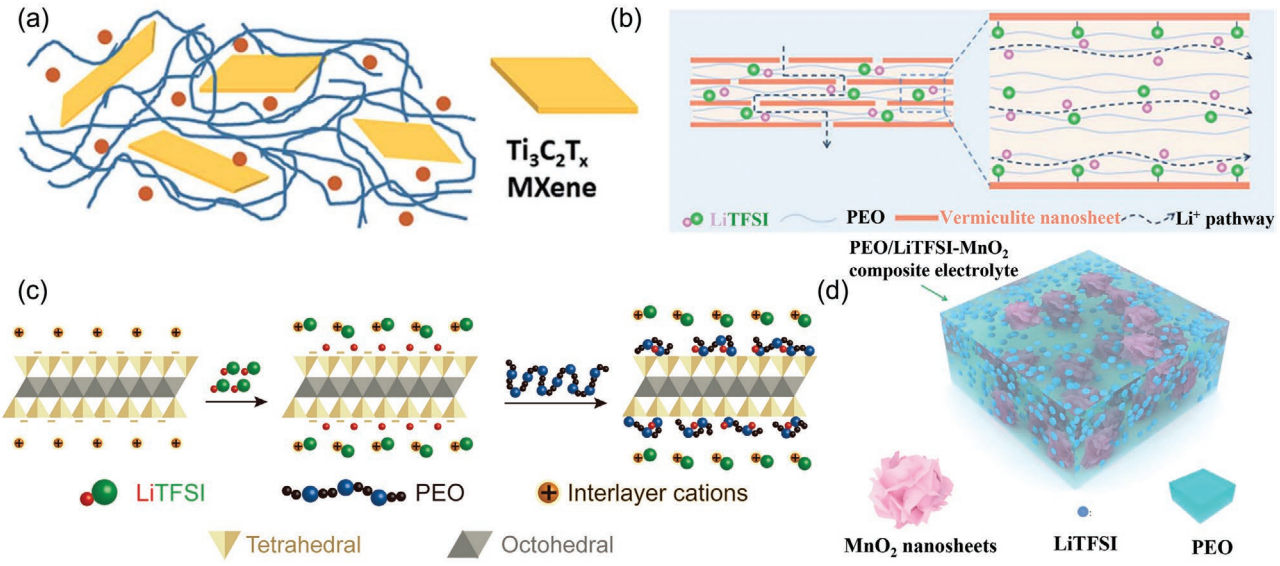

Figure 7. a) MXene/PEO composition polymer electrolytes (CPEs). Reproduced by permission.[155] Copyright 2020, American Chemical Society. b) The lithium ions transfer mechanism in Vr/PEO-LCSE. Reproduced by permission.[156] Copyright 2020, Royal Society of Chemistry. c) Mechanism for VS enhanced ionic conductivity in SPE. Reproduced by permission.[157] Copyright 2019, American Chemical Society. d) Composition of a PEO/LiTFSI/MnO_2 solid polymer electrolyte membrane. Reproduced by permission.[158] Copyright 2020, Royal Society of Chemistry.

© 2022 Wiley-VCH GmbH

crystallinity of the PEO, which enhances the ionic conductivity. Moreover, the dissociation of lithium salt can be enhanced by the Lewis acid-base interactions between Ni atoms in NMS and anions in the lithium salt, which can increase the concentration of Li-ion in PEO. The Li-ion transference value reaches to 0.378 and the ionic conductivity reaches 1.66×10^{-5} S cm^{-1} at 25 °C. Similar with other 2DMs, NMS can enhance the mechanical strength of the PEO. At 0.1 C at 30 °C after 50 cycles, the all-solid-state Li/$LiFePO_4$ battery with NMS/PEO shows a high reversible capacity of 130 mA h g^{-1}.[155]

Second, with the application of 2DMs, the mechanical strength of PEO can be enhanced significantly. 2D BN can be also used in polymer solid electrolyte due to its excellent electrochemical properties. Based on the conventional properties of 2D BN, Zhang et al. designed a new ASSLB based on boron nitride enhanced polymer/salt (PVDF-HFP/LiTFSI) composite electrolytes. By the application of the 2D BN, the mechanical strength, ionic conductivity, and interface contact of the composite electrolyte was enhanced. The ionic conductivity of 1% BN composite electrolyte is 1.82×10^{-3} S cm^{-1} at room temperature. In order to test the mechanical strength of composite electrolyte, the hardness and Young's modulus were tested, which is 4.99 MPa and 0.133 GPa, relatively, which can significantly suppress the growth of lithium dendrites.[161] Furthermore, Yin et al. proposed the importance of thermal uniformity for SSEs. After the addition of 2D BN, BN-PEO-PVDF's ionic conductivity and mechanical strength were improved significantly. Specially, 2D BN enables fast conduction and uniform distribution of heat in PEO. As a result, homogenous ionic conductivity is achieved in PEO, because the ionic conductivity of PEO depends on temperature. Finally, The deposition and extraction of lithium become more uniform, and thus the ASSLBs show long cycle life and high performance.[162] In order to significantly improve the mechanical properties of PEO, Zhai et al. applied vermiculite nanosheets into PEO to fabricate Vr/PEO-LCSE. At 25 °C, the Vr/PEO-LCSE shows a high ionic conductivity of 1.22×10^{-5} S cm^{-1} (Figure 7b). The specific resistance of Vr/PEO-LCSE is much lower than pure PEO which is 66 Ω cm^{-2} at 30 °C. In addition, the excellent compressive strength of Vr/PEO-LCSE is 131 MPa which is much higher than pure PEO and compared with other 2DM additives. As result, the high-rate performance of ASSLBs is improved, which has low capacity fading from 0.05C to 0.2C.[156]

Third, 2DMs such as 2D VS, lepidolite can provide extra ionic transport channels to enhance the ionic conductivity. Due to the high specific properties, most 2DMs can make fast lithium-ion transport on the surface. To be specific, the properties of VS are similar with inactive ceramic fillers, VS has high chemical, thermal, machinal stability. Furthermore, the negative charge surface of the VS can be used to transport Li-ions. In order to study the effect of 2D material arrangement on lithium-ion transmission, Tang et al. first fabricated a PEO/LiTFSI/10% 2D VS layered composition electrolyte to improve the electrochemical performance of ASSLBs with disorderly arrangement (Figure 7c). The Negatively charged surface of 2D VS layers provide more channels for lithium-ion transport. Thus, the lithium-ion conductivity is much higher than normal PEO. At 25, 60, and 100 °C, the ionic conductivity is 2.9×10^{-5}, 1.2×10^{-3} and 3.1×10^{-3} S cm^{-1}, respectively. In addition, at current density of 50 μA cm^{-2}, the Li/VS composition PEO/Li symmetrical cells work with stable voltage profiles over two months. The Li/$LiFePO_4$ cell is tested in this time, at 0.1 C and 0.5 C, the capacity of this battery is 159.9 and 152.0 mA h g^{-1}, respectively.[163] In addition, Tang et al. designed another ASSLB using 2D VS layers. In this time, 2D VS is arranged in PEO in a vertical direction, which can generate continuous channels and larger surface area. As a result, Li^+ transference number close to 0.5 reaches an ionic conductivity as high as 1.89×10^{-4} S cm^{-1} at 25 °C.[164,165] A lithium symmetric battery using vertically aligned VS-based PEO composite electrolyte was tested over 1300 h, which is stable with low overpotential.[166] The full battery test was also tested here to verify the performance of this electrolyte, at 0.1 C, 35 °C, the ASSLBs based $LiFePO_4$ showed a capacity of 167 mA h g^{-1} with the application VAVS–CSPE and retains 82% capacity after 200 cycles at 0.5 C.[164,167] PEO has shown improved thermal stability, high mechanical strength, ionic conductivity, and electrochemical stability after the addition of 2D VS layers, and decreased flammability and interface resistance.[157]

Covalent nitrides with high thermal and chemical stability are always applied to stabilize the interface between the PEO-based electrolyte and lithium metal anode. By the application of nitrides in PEO, the highly electronegative N atoms will interact with $TFSI^-$ to enhance the and selectivity of ion transport and dissociation of LiTFSI in PEO. First example is for selectivity of ion transport. Li et al. applied 2D hexagonal boron nitride (h-BN) in PEO. The stronger binding effect between $TFSI^-$ and BN than between Li-ion and BN is simulated by the density-functional theory (DFT) calculation, which indicates that the Li-ion conductivity of PEO/LiTFSI/BN is lower than without BN. However, the transport of $TFSI^-$ is reduced significantly. As a result, with the application of h-BN, the selectivity of Li-ion transport is higher. The Li/Li symmetric battery with PEO/LiTFSI/h-BN lasts 430 h at 0.2 mA cm^{-2}. For the full battery with Li metal anode and $LiFeO_4$ cathode, the PEO/LiTFSI/h-BN composite electrolyte shows great cycle life for 140 cycles, compared to 39 cycles for SSEs without the addition of h-BN.[168] Second example is for enhancing the dissociation of LiTFSI. g-C_3N_4 nanosheets have some defects on the surface which is different with other defects in the other 2DMs, as it can provide extra lithium transport channels. In order to improve the performance of PEO, Sun et al. added g-C_3N_4 nanosheets into the PEO to improve the ionic conductivity, working temperature and mechanical strength. The ionic conductivity reaches 1.7×10^{-5} S cm^{-1} at 30 °C. Moreover, lithium salt can interact with the N atoms on the surface of g-C_3N_4 nanosheets to improve the dissociation of the lithium salt. After 100 cycles, at 60 °C, the ASSLBs with PEO/g-C_3N_4 nanosheets show 155 mA h g^{-1}.[169]

Naturally derived 2DMs have also been explored as a PEO additive. Wang et al. reported one kind of 2D natural layered silicate material, lepidolite. They designed a composite electrolyte with lepidolite, PEO and $LiClO_4$. The pure lepidolite is tested first, it has an ionic conductivity at 100 °C of 1.5×10^{-5} S cm^{-1}. The composition with PEO and lepidolite without Li salt was tested next, it shows an increased Li-ion transference number with larger content of lepidolite in the composites. In order to increase the interface contact and ionic conductivity, PEO and

© 2022 Wiley-VCH GmbH

15214095, 2022, 16, Downloaded from https://onlinelibrary.wiley.com/doi/10.1002/adma.202108079 by Xian Jiaotong University, Wiley Online Library on [06/06/2024]. See the Terms and Conditions (https://onlinelibrary.wiley.com/terms-and-conditions) on Wiley Online Library for rules of use; OA articles are governed by the applicable Creative Commons License

$LiClO_4$ were added into the lepidolite to form the composite electrolytes, and the ionic conductivity at 60 °C can be increased to 1.6×10^{-4} S cm^{-1}. The obtained CPEs show improved ionic conductivity, greater Li^+ transfer, higher thermal stability and better mechanical characteristics than traditional polymer electrolytes.[157] Compared to other 2DMs, the combination between PEO and MnO_2 can provide long-range migration for lithium ions. Li et al. applied MnO_2 into PEO to produce PEO/MnO_2 electrolyte, which exhibits better ionic conductivity, lithium transference number, and mechanical strength (Figure 7d). By density functional theory calculations, the PEO/Li complex and MnO_2 binding energy is small, which is beneficial for lithium ion to transfer in the interface between PEO and MnO_2. After 300 cycles, the ASSLB with PEO/MnO_2 electrolyte exhibits 143.5 mA h g^{-1}.[158]

Finally, the application of 2DMs is used to improve the thermal uniformity of PEO-based polymer electrolytes to stabilize the ASSLBs at high temperature. Yin et al. applied 2D BN nanoflakes to deal with high operating temperature, poor thermal conductors, and lithium deposition problems in ASSLBs. After the addition of 2D BN, BN-PEO-PVDF's ionic conductivity, mechanical strength, and heat transport ability was improved significantly. Specially, 2D BN enables fast conduction and uniform distribution of heat in PEO. Finally, The deposition and extraction of lithium become more uniform, and thus the ASSLBs shows long cycle life, and high electrochemical performance.[162] (**Table 1**).

3.2.2. Other Solid Polymer Electrolytes

Besides PEO, other polymers such as PAN, PVDF, etc., have also been used as the solid electrolyte. 2D single-layer GO is one of the potential materials for application in ASSLBs. It has a large specific surface area and many oxygen-containing functional groups. It has been reported that the application of GO can enhance the transport of Li-ions and the chemical stability of the electrolyte, which is due to the oxygen-containing functional groups and the 2D structure of GO. Jia et al. reported a new design of $LiClO_4$-polyacrylonitrile (PAN) SPEs with the application of GO. This GO is modified by −OH, −COOH, −COC, and other oxygen-containing functional groups. At 30 °C, the ionic conductivity of composite PAN electrolyte with 1 wt% GO reached 4.0×10^{-4} S cm^{-1}, which is higher than pure PAN (2.2×10^{-5} S cm^{-1}). In addition, the application of GO reduces the activation energy from 2.31 to 1.03 eV and increase the tensile modulus from 37 to 80 MPa. Moreover, GO makes the polymer less crystalline to have better contact with the electrode. In terms of electrochemical performance, the $LiFePO_4$ (LFP) battery with 1.0 wt% GO-SPE as the electrolyte has an average discharge capacity of 166 mA h g^{-1} when maintained at 0.2 C for 50 cycles, and the electrochemical polarization is relatively small at 38 mV.[170]

Table 1. The contribution of 2DMs to ionic conductivity of PEO based electrolyte.

Materials*	Ionic conductivity [S cm^{-1}]	Temperature [°C]	Ref
Polyethylene oxide	10^{-6}–10^{-8}	25	126
MXene	2.2×10^{-5}	28	155
Polyethylene glycol-grafted graphene	2.53×10^{-5}	30	159
Vermiculite sheets	2.9×10^{-5}	25	
	1.2×10^{-5}	60	
	3.1×10^{-5}	100	163
Vertically aligned vermiculite sheets	1.89×10^{-4}	25	164
Lepidolite	1.6×10^{-4}	60	157
Nickel-based ultrathin MOF nanosheets	1.66×10^{-5}	25	155
Boron nitride	1.82×10^{-3}	25	161
g-C_3N_4 nanosheets	1.7×10^{-5}	30	169
Vermiculite nanosheets	1.22×10^{-5}	25	156

3.2.3. Solid Sulfide Electrolytes

Compared with SPEs, solid sulfide electrolytes (SSEs) can potentially combine the advantages of polymer electrolytes and oxygen-containing electrolytes. They have medium mechanical strength, which is favorable for both the interface contact and structural stability. However, SSEs are not chemically stable, as side reactions low coulombic efficiency. In this section, some improvement strategies will be introduced by the application of 2DMs. It can be divided into two parts.

One is mitigating the side reactions. Xu et al. designed a strong $Li_7P_3S_{11}$ electrolyte with BN doping for an all-solid-state lithium sulfur battery (**Figure 8**a). The BN nanosheets is able to partially separate the $Li_7P_3S_{11}$ solid electrolyte and lithium metal, thereby enhancing the electrode and electrolyte interfacial performance and prevent $Li_7P_3S_{11}$ from reacting with Li metal. By the application of boron nitride doped $Li_7P_3S_{11}$ solid electrolyte, this ASSLB shows improved electrochemical performance with better cycling stability and higher coulombic efficiency.[171,172]

Another one is providing extra lithium-ion transport channels. TiS_2 is one kind of TMDs. To deal with the poor ionic contacts between the active material and sulfide solid electrolyte, Oh et al. applied TiS_2 nanosheets which is prepared by the scalable mechanochemical lithiation to prepare TiS_2, followed by exfoliation by ultrasonication to prepare the nanosheets (Figure 8b). With the addition of TiS_2, ASSLBs shows excellent reversible capacity due to the favorable contact with TiS_2 nanosheets and short lithium-ion transport channel. Compared with bulk TiS_2, TiS_2 nanosheets show shorter Li-ion transport channels and high electronic conductivity.[173]

3.2.4. Other Type of Solid-State Electrolytes

Besides the solid polymer electrolyte, sulfide solid electrolyte, and solid oxide electrolyte, there are also many novel materials used as solid electrolytes. In this section, the application of 2DMs can be divided into two parts.

As usual, 2DMs provide extra lithium ionic transport channel to enhance the ionic conductivity of the electrolyte. Due to its porous structure and functionalization, perovskite

© 2022 Wiley-VCH GmbH

15214095, 2022, 16, Downloaded from https://onlinelibrary.wiley.com/doi/10.1002/adma.202108079 by Xian Jiaotong University, Wiley Online Library on [06/06/2024]. See the Terms and Conditions (https://onlinelibrary.wiley.com/terms-and-conditions) on Wiley Online Library for rules of use; OA articles are governed by the applicable Creative Commons License

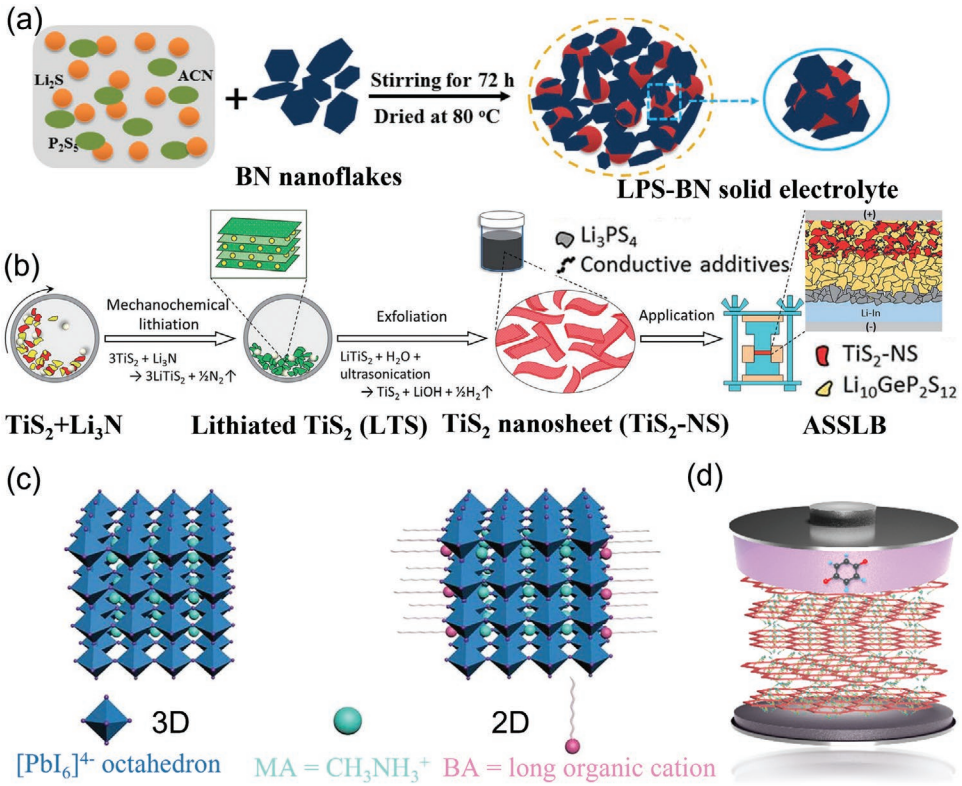

Figure 8. a) Fabrication process of LPS-BN solid electrolyte. Reproduced by permission.[171] Copyright 2019, Springer Nature. b) preparation of TiS_2 nanosheets (TiS_2-NSs) and their application in bulk-type ASSLBs using sulphide SEs. Reproduced by permission.[173] Copyright 2016, Royal Society of Chemistry. c) Crystal structure of the 3D-PVSK and 2D-PVSK. Reproduced by permission.[175] Copyright 2020, Wiley-VCH. d) 2D COF solid state electrolyte. Reproduced by permission.[178] Copyright 2020, American Chemical Society.

and COF can be used as the electrolyte to promote the lithium-ion transport. Wu et al. use two kinds of perovskites: 3D-PVSK (CH_3NH_3PbI) and 2D-PVSK ($BA_2MA_3Pb_4I_{13}$) to modify the surface of the $Li_{6.75}La_3Zr_{1.75}Ta_{0.25}O_{12}$ (LLZTO) (Figure 8c). With the modification of 3D-PVSK and 2D-PVSK, 2D PVSK provides extra transport channels for Li-ions compared with other modification methods. ASSLBs use lithium as the anode and $LiFeO_4$ as the cathode to test the application of 2D PVSK. The results show that ASSLBs have higher specific capacities of 153 and 149 mA h g^{-1} with 3D-PVSK and 2D-PVSK respectively compared with no-PVSK ASSLBs, after 50 cycles at 0.2 C. To sum up, with the modification of 3D-PVSK and 2D-PVSK, it will provide more lithium storage of ASSLBs.[174] Li et al. designed a new dCOF with TFSI functional group (dCOF-ImTFSI-60). By the postfunctionalization of $TFSI^-$, the ionic conductivity of dCOF-ImTFSI-60 is 7.05 $\times$ 10^{-3} S cm^{-1} at 423 K with the extra 1D pores for lithium ionic transport by the extra $TFSI^-$. Li/dCOF-ImTFSI-60@Li/$LiFePO_4$ ASSLB shows an initial capacity is 143.7 mA h g^{-1} under 353 K and retains 98.3% capacity after 40 cycles with 97.5% coulombic efficiency.[175]

In addition, dCOF will have a wide range working temperature range from 303 to 423 K.[175] In the other work, Li et al. designed another type of 2D COF (Im-COF-Br) which was synthesized by Schiff base reaction, and the building block is imidazolium-based monomers. This new COF has some characteristics, such as positive charge in the COF skeletons, tunable counter-anions, and 5.57 nm pore sizes. In order to increase the transport of Li-ion, the Br^- is replaced with TFSI. The Im-COF-TFSI was tested at 353 and 423 K, which shows ionic conductivities of 4.64 $\times$ 10^{-4} and 4.04 $\times$ 10^{-3} S cm^{-1}, respectively.[176] Zheng et al. designed a new combination between COF and PEO to fabricate a new type of electrolyte, which flexible and ethylene oxide PEO in the rigid 2D COF architectures is used as lithium ionic transport channel to enhance the Li-ion conductivity. It is verified by powder X-ray diffraction and thermogravimetric analysis that the periodic structure is stable even over 300 °C, and the dynamic glassy structure of PEO is verified by differential scanning calorimetry and NMR. The Li-ion conductivity reaches 1.33 $\times$ 10^{-3} S cm^{-1} at 200 °C with LiTFSI doping.[177]

On the other hand, 2DMs are also applied as the electrolyte to transport lithium ions individually. Li et al. applied 2D lithiated hydrazone-based COF with phenol group (2D LiCON) nanosheets into ASSLBs (Figure 8d). First, at 40 °C, the ionic conductivity of COF without Li salt reaches 10^{-5} S cm^{-1}. Second, it prevents the dissolution of organic redox species in the cathode. When the 2D LiCON is applied in the ASSLB, it is stable for 500 cycles at 500 mA g^{-1} at 20 °C.[178] In addition, with the unique properties of 2D COF, Sun et al. fabricated ultrathin SSEs with a thickness of 7.1 µm, which contributes to the high energy density of the battery.[179]

© 2022 Wiley-VCH GmbH

15214095, 2022, 16, Downloaded from https://onlinelibrary.wiley.com/doi/10.1002/adma.202108079 by Xian Jiaotong University, Wiley Online Library on [06/06/2024]. See the Terms and Conditions (https://onlinelibrary.wiley.com/terms-and-conditions) on Wiley Online Library for rules of use; OA articles are governed by the applicable Creative Commons License

4. Emerging Advanced Characterizations for 2DMs Used in ASSLBs

Considering the specific 2D structure and physicochemical properties of 2DMs, only a few emerging advanced characterization technologies will be focused on this section to deeper the understanding of the structure–function relationship in 2DMs for ASSLBs. The advanced characterizations including synchrotron X-ray techniques and in situ/operando characterization are summarized below.

Synchrotron radiation is one of the most powerful technologies to study the structure and mechanism of battery materials. Compared with traditional characterization technologies, with the assistant of the high flux and brilliant X-ray beam, there are some advantages. First, it can get high structural resolution and 2D/3D morphology of 2DMs in ASSLBs due to the low presence of 2DMs in ASSLBs. Second, it has high temporal resolution, it can significantly shorten the time required for signal acquisition to get the dynamic information of 2DMs with combination with in-situ/operando technology. Third, direct visualization and 3D reconstruction of 2DMs can be acquired at the same time. In conclusion, in order to gain an in-depth understanding of the effect of 2DMs in the electrolyte, electrode, and interface of ASSLBs, the synchrotron X-ray technique plays a critical role, which can be divided into four parts: XRD, X-ray absorption fine structure (XAFS), X-ray photoelectron, and X-ray microscopy. In order to investigate the state of ASSLBs in the dimensions of time and space during operation, in-situ/operando technologies are applied as one of the most necessary technology to monitor energy-storge mechanisms with ASSLBs.[180,181]

In-situ characterization is applied to obtain the structure and composition information of the sample most truthfully. With the application of the in-situ characterizations, the influence on the sample during the sample preparation process is avoided. After by optimizing the in-situ cell, operando technology is applied to achieve real-time observation of changes in ASSLBs. As a results, in-situ/operando technology is one of the most important characterization technologies for study of 2DMs in the ASSLBs.

In this section, spectroscopy material composition analysis and morphology and structure characterization will be introduced.

4.1. Spectroscopy Material Composition Analysis

With the assistant of X-ray technology, in the structural investigations of SSEs, synchrotron XRD is one of the most attractive methods to obtain the structure and chemical information of SSEs. In contrast to laboratory X-ray sources, the measurement of scattering from dilute phases or the analysis of residual stress can be obtained by the assistance of the high resolution and intensity of the synchrotron.[182,183] In addition, synchrotron radiation has the unique advantages of enhancing the signal strength and reducing test time, which enables the development of time-resolved XRD and in situ/operando XRD in synchrotron beamlines. Thus the crystallographic information of 2DMs, including lattice parameters of different phases, site occupancy, strain/stress, and microstructural information, can be further detected by the diffraction techniques.[184–186]

As mentioned above, the interface stability of interface between the electrolyte and electrode is one of the essential problems that should be resolved, especially for high-voltage cathode materials, such as $LiCoO_2$. To detect the side reactions during operation, in situ XRD is applied in here. For instance, Vardar et al. applied $LiCoO_2$ electrode and LLZO electrolyte as a model system. The side reaction products are easily detected by the application of synchrotron source, new peaks were detected which is attributed to the composition of Li_2CO_3, $La_2Zr_2O_7$, and $LaCoO_3$ (**Figure 9**a). The side production layer will suppress the lithium-ion transport in the interface.[187] With the assistance of 2DMs at the cathode electrolyte, the side reactions between electrolyte and high-voltage cathode has been significantly suppressed. Through synchrotron radiation in-situ XRD monitoring, any side-products produced by the electrode and electrolyte in the operation process can be immediately observed to analyze the failure mechanism of ASSLBs.

XAFS is one of the most powerful technical tools for analyzing 2DMs. It describes X-ray absorption near or above the absorption edge. Due to the different energy ranges, XAFS can be divided into two parts. X-ray near-edge absorption structure (XANES) refers to the spectral region from the absorption edge to the energy range of 30–50 eV beyond the absorption edge. Extended X-ray absorption fine structure (EXAFS) is a type of extended X-ray absorption fine structure. XANES can distinguish between electronic states and 3D coordination geometry. Differently, EXAFS is sensitive to the distance, coordination number, and type of atoms around the adsorbed atoms.[188]

To distinguish the difference of the local atomic geometry and the chemical state of the atoms for 2DMs with their 3D bulk counterparts, XAFS is applied to analyze the specific element. For example, for the atom of a specific element, the coordination number is significantly reduced, and bond lengths are elongated in 2DMs compared with the bulk materials.[189] For the ASSLBs, the presence of 2DMs in electrode and electrolyte are minimal. To detect the 2DMs, with the application of synchrotron radiation, the X-ray absorption energy near or above the absorption edge can be detected. In addition, compared with the EXAFS, the signal of XANES is clearer, the time required to collect the signal is shorter, and it is more sensitive to the element valence and charge transfer.

Therefore, the in situ XANES based on the synchronous light source has a time resolution that can be used to study the electronic states and 3D coordination geometry of specific elements for 2DMs in ASSLBs. [190] To analyze the failure mechanism of the SSEs, Li et al. applied in situ XANES to observe the nanoscale molecular level and local chemical environment in real time during the operation state of SSE-Li_3InCl_6 (Figure 9b). As a result, the degradation reaction can be observed between H_2O and Li_3InCl_6, which will produce In_2O_3 and LiCl to reduce the ionic conductivity of SSE.[191]

In summary, by the application of in situ characteristics technology and synchrotron radiation technology of XAFS, changes in the coordination environment of any element can be observed under operating conditions of ASSLBs, which is of great significance for the more detailed interpretation of the application of characteristic elements in 2DMs in ASSLBs.[192]

© 2022 Wiley-VCH GmbH

15214095, 2022, 16, Downloaded from https://onlinelibrary.wiley.com/doi/10.1002/adma.202108079 by Xian Jiaotong University, Wiley Online Library on [06/06/2024]. See the Terms and Conditions (https://onlinelibrary.wiley.com/terms-and-conditions) on Wiley Online Library for rules of use; OA articles are governed by the applicable Creative Commons License

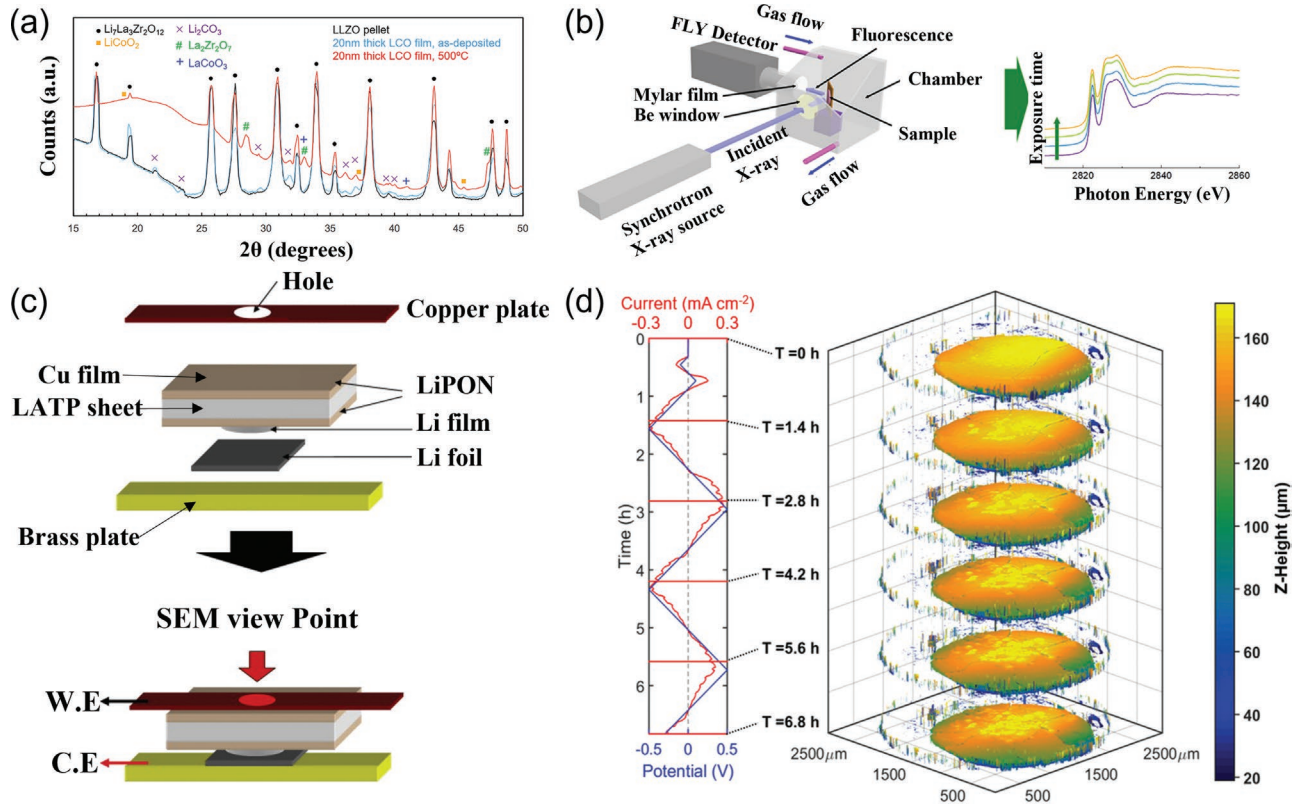

Figure 9. Advanced synchrotron/in situ characterization a) in-situ XRD to detect side-production in the interface between $LiCoO_2$ electrode and LLZO electrolyte. Reproduced by permission.[187] Copyright 2018, American Chemical Society. b) In situ XANES to detect degradation reaction of Li_3InCl_6. Reproduced by permission.[191] Copyright 2020, American Chemical Society. c) In situ SEM to characterize growth of lithium metal dendrites. Reproduced by permission.[196] Copyright 2013, Elsevier. d) In situ X-ray tomography to monitor the real-time 3D morphology of the LGPS solid electrolyte. Reproduced by permission.[197] Copyright 2020, Wiley-VCH.

Lithium metal is prone to irreversible side reactions with solid electrolytes due to its high reactivity, leading to battery failure. Therefore, it is of great significance to construct an interface layer with high ionic conductivity. In situ XPS is one technique to delineate the composition change of the SEI during the charge and discharge process. Janek et al. used in situ XPS to characterize the electrochemical deposition process of lithium metal on the surface of a typical sulfide solid electrolyte $Li_{10}GeP_2S_{12}$ (LGPS) to study the interface stability of the LGPS and lithium metal. According to the known position and intensity of the peaks of the relevant components, by fitting the in situ XPS peaks, it is possible to compare and observe the changes of each component during the charging and discharging process.[193] Yan et al. applied the BN nanosheet as SEI to suppress the side-reaction between electrolyte and lithium metal. In situ XPS can be used in here to detect the SEI composition in the operation process, the content change of Li_3N during lithium deposition can be detected.[125]

4.2. Morphology and Structure Characterization

The mechanism of in situ TEM is that the electron beam with a very short wavelength penetrates the sample and uses an electromagnetic mirror to control the focus of the electron beam to measure it. In situ TEM improves the time-based resolution to detect the microscopic morphology, crystal structure and phase, which is one of the powerful analytical methods for systematically studying the electrochemical reaction mechanism and failure mechanism of the solid-state battery charge and discharge process. Nomura et al. used the EELS of the TEM to use sparse coding and structure technology to dynamic change of the lithium ions concentration distribution in SSE. Dynamic observation found that during the electrochemical reaction, lithium ions not only move in the vertical direction to the SEI, but also move in parallel directions, resulting in spatial changes in the concentration of lithium ions on the nanometer scale. With the addition of 2DMs in the SSE, the lithium ions concentration distribution in the interface between SSE and 2DMs will represent the unique lithium ions transport way by the observation of in situ TEM.[194]

In situ SEM technology is based on the secondary electrons and scattered electrons when electron beam scans the surface of the sample to obtain the real-time imaging. In addition, with the assistant of EDS, the element changes during the charge and discharge process. In ASSLBs, the growth of lithium dendrites in the lithium metal anode is one of the most serious problems. The application of 2DMs, such as MXene, BN, VS, etc., in the interface between the anode and electrolyte is used to suppress the growth of lithium dendrites, as it changes the

© 2022 Wiley-VCH GmbH

15214095, 2022, 16, Downloaded from https://onlinelibrary.wiley.com/doi/10.1002/adma.202108079 by Xian Jiaotong University, Wiley Online Library on [06/06/2024]. See the Terms and Conditions (https://onlinelibrary.wiley.com/terms-and-conditions) on Wiley Online Library for rules of use; OA articles are governed by the applicable Creative Commons License

15214095, 2022, 16, Downloaded from https://onlinelibrary.wiley.com/doi/10.1002/adma.202108079 by Xian Jiaotong University, Wiley Online Library on [06/06/2024]. See the Terms and Conditions (https://onlinelibrary.wiley.com/terms-and-conditions) on Wiley Online Library for rules of use; OA articles are governed by the applicable Creative Commons License

mechanism of the growth of lithium metal.[195] As a result, the application of in situ SEM is important to observe the whole process of growth of lithium dendrites. Sagane et al. applied LiPON ($Li_{3.3}PO_{3.8}N_{0.22}$) as the SSE and performed in situ SEM to observe the process of extraction and deposition of lithium metal on the surface of the negative electrode (Figure 9c). With the application of 2DMs such as MXene, BN, VS, in the interface between anode and electrolyte to suppress the growth of lithium dendrites, the mechanism of the growth of lithium metal is different.[196]

In situ X-ray tomography can track the dynamic changes of the morphology, crystal structure, and chemical components of the components in the battery in real time during battery operation, which is of great significance for the study of solid-state battery interface properties, interface changes, and battery failure mechanism. Gewirth et al. constructed Li|LGPS|Li symmetrical battery and used in situ X-ray tomography to monitor the real-time 3D morphology of the LGPS solid electrolyte, especially the interface between the LGPS and lithium metal during the battery cycle (Figure 9d). Compared with polymer-based solid electrolyte, in situ X-ray tomography is more important for oxygen-based and sulfur-based electrolytes, the arrangement mode of the particles will have a huge impact on the conduction of lithium ions.[197]

Aside from summarized technologies, some other advanced characterizations are also applied in the 2DMs used in ASSLBs, such as cryo-electron microscopy, spherical aberration electron microscopy, et al.

5. Summary, Challenges, and Perspectives

5.1. Summary

Although one of the most mature battery technologies, lithium batteries still have many aspects that have not reached the desired requirements, such as energy density, current density, safety, environmental compatibility, and price. Through the combination of characterization technology, 2DMs, and advanced fabrication method, ASSLBs have gradually approached liquid lithium batteries in terms of electrochemical performance. Overall, advanced characterization technology has continuously deepened the understanding of 2DMs, and the application of 2DMs in ASSBLBs has also become diversified, playing different roles in different components.

5.2. Challenges and Perspectives

Despite the advanced and increasing research work of 2DMs in ASSLBs summarized in this review, the application of 2DMs in ASSLBs is still in the initial state. There are still many serious problems in the practical application of ASSLBs, such as lithium-ion transport, high interface resistance, and side production. In order to maximize the role of 2DMs in ASSLBs, some proposed directions are discussed below.

(1) Modification of 2DMs

2DMs can be modified by multiple methods such etching and surface functionalization to further improve the electrochemical performance. In the research mentioned in the review, most 2DMs are applied directly in the ASSLBs. As a result, in order to maximize the role of 2DMs in ASSLBs, it is necessary to investigate the relationship between modification and electrochemical performance. For ASSLBs, it is mostly considered for improvement for the lithium metal battery which has highest energy density in lithium battery. For the anode side, it is necessary to enhance the chemical stability, mechanical strength of 2DMs to suppress the side-reaction between lithium metal anode and growth of the lithium dendrites. For the cathode side, it is little study on the high-voltage cathode material such like: $LiNi_{0.8}Co_{0.1}Mn_{0.1}O_2$, $LiCoO_2$, et al. on the ASSLBs. It is important to modify the 2DMs to deal with side-reaction between high-voltage cathode material and electrolyte. After solving this problem, it can further improve the energy density of ASSLBs. For electrolyte, modified 2DMs can provide a comprehensive solution to the low ion conductivity of ASSLBs at room temperature, especially polymer-based solid electrolytes.

(2) In situ/operando characterization of the lithium-ion transport of 2DMs in SSEs

In situ/operando characterization technology can enhance scientists' understanding of the nature of some phenomena in ASSLBs. For electrolyte, since the introduction of solid lithium-ion conductors, the current mechanism of lithium-ion transport based on pure SSEs has been interpreted by various models. However, with addition of 2DMs, the mechanism of lithium-ion transport in the SSEs has been adjusted, which is necessary to understand the difference of the mechanism of lithium-ion transport in the SSEs with/without the addition of 2DMs. To achieve this goal, advanced methods, such as in situ/operando neutron depth profiling (NDP), X-ray tomographic microscope (XTM), and simulation methods such as DFT and ab initio molecular dynamics (AIMD) could analyze the composite material systems, which should be applied here to analyze the mechanism of lithium-ion transport. For the interface problem between electrolyte and anode, in situ/operando characterization can be applied to reveal the change of the interface component morphology during the battery operation, to take corresponding measures to improve the interface dynamics of the ASSLBs.

(3) Development of Novel 2DMs

Although current 2DMs play an important role in ASSLBs, the novel 2DMs with excellent electrochemical activity should be continually developed. For instance, in the anode side, 2DMs with higher ionic conductivity and higher mechanical strength should be discovered. In the cathode side, novel 2DMs should have higher electronic conductivity and theoretical capacity. In the electrolyte, 2DMs require higher ionic conductivity, higher mechanical strength, etc. Based on the different requirements for different components of ASSLBs, machine learning and artificial intelligence can be very effective means to predict the application of new 2DMs for ASSLBs. These two technologies

 © 2022 Wiley-VCH GmbH

can greatly reduce the time required for people to screen materials in the early stage, which continues to promote the application of new 2DMs.

In conclusion, the application of 2DMs in ASSLBs is still preliminary. To promote the practical development of ASSLBs, more kinds of 2DMs and characterization methods for different aspects need to be further developed. With the assistance of new 2DMs and novel material fabrication method for ASSLBs, the application of 2DMs for the practical application of ASSLBs will be extended. The development of advanced characterization further reveals the failure mechanism of ASSLBs, which provides targeted guidance and ideas for 2DMs to solve the current problems encountered by ASSLBs. In short, the combination of 2DMs and ASSLBs is a hotspot for research and practical applications. This work will promote the rapid development of next-generation lithium batteries-ASSLBs to replace the current technology dominated by liquid batteries.

Acknowledgements

Q.M. and Y.Z. contributed equally to this work. This work was supported by the Department of Science and Technology of Guangdong province (No. 2020B0909030004), the Cultivation Foundation of South China Normal University for Young Teachers (No. 20KJ09) Science and Technology Program of Guangzhou (No. 2019050001), the fellowship of China Postdoctoral Science Foundation (Nos. 2021M691091 and 2021M691087). The authors thank the support from the Program for the Natural Sciences and Engineering Research Council of Canada, Mathematics of Information Technology and Complex Systems (Mitacs), University of Waterloo and Waterloo Institute for Nanotechnology. The authors are grateful for the technical support for Nano-X from Suzhou Institute of Nano-Tech and Nano-Bionics, Chinese Academy of Sciences (SINANO).

Conflict of Interest

The authors declare no conflict of interest.

Keywords

2D materials, all-solid-state lithium batteries, lithium metal anodes, solid electrolytes

Received: October 8, 2021
Revised: December 15, 2021
Published online: February 26, 2022

[1] J. A. Parellada, M. M. Dunn, A. Wayland, J. Cousins, E. Shaw de Paredes, *Appl. Radiol.* **1997**, *26*, 7.
[2] A. Manthiram, *J. Phys. Chem. Lett.* **2011**, *2*, 176.
[3] A. Manthiram, Y. Fu, Y. S. Su, *Acc. Chem. Res.* **2013**, *46*, 1125.
[4] J. Wang, Y. Yamada, K. Sodeyama, E. Watanabe, K. Takada, Y. Tateyama, A. Yamada, *Nat. Energy* **2018**, *3*, 22.
[5] C. Sun, J. Liu, Y. Gong, D. P. Wilkinson, J. Zhang, *Nano Energy* **2017**, *33*, 363.
[6] M. Li, J. Lu, Z. Chen, K. Amine, *Adv. Mater.* **2018**, *30*, 1800561.
[7] M. A. Hannan, M. S. H. Lipu, A. Hussain, A. Mohamed, *Renewable Sustainable Energy Rev.* **2017**, *78*, 834.
[8] R. C. Xu, X. H. Xia, S. Z. Zhang, D. Xie, X. L. Wang, J. P. Tu, *Electrochim. Acta* **2018**, *284*, 177.
[9] S. Chen, D. Xie, G. Liu, J. P. Mwizerwa, Q. Zhang, Y. Zhao, X. Xu, X. Yao, *Energy Storage Mater.* **2018**, *14*, 58.
[10] S. S. Zhang, *J. Power Sources* **2013**, *231*, 153.
[11] F. Zheng, M. Kotobuki, S. Song, M. O. Lai, L. Lu, *J. Power Sources* **2018**, *389*, 198.
[12] P. Albertus, S. Babinec, S. Litzelman, A. Newman, *Nat. Energy* **2018**, *3*, 16.
[13] W. Li, H. Yao, K. Yan, G. Zheng, Z. Liang, Y. M. Chiang, Y. Cui, *Nat. Commun.* **2015**, *6*, 7436.
[14] G. Xu, B. Ding, J. Pan, P. Nie, L. Shen, X. Zhang, *J. Mater. Chem. A* **2014**, *2*, 12662.
[15] M. Armand, *Nature* **2001**, *414*, 359.
[16] Y. Liu, P. He, H. Zhou, *Adv. Energy Mater.* **2018**, *8*, 1701602.
[17] X. Judez, H. Zhang, C. Li, G. G. Eshetu, J. A. González-Marcos, M. Armand, L. M. Rodriguez-Martinez, *J. Electrochem. Soc.* **2018**, *165*, A6008.
[18] L. Xu, S. Tang, Y. Cheng, K. Wang, J. Liang, C. Liu, Y. C. Cao, F. Wei, L. Mai, *Joule* **2018**, *2*, 1991.
[19] H. Tao, J. Li, Q. Ma, Z. Chen, X. Zhang, Y. Quan, P. Yang, C. Qi, *Chem. Eng. J.* **2020**, *382*, 123045.
[20] A. Varzi, R. Raccichini, S. Passerini, B. Scrosati, *J. Mater. Chem. A* **2016**, *4*, 17251.
[21] J. Wan, J. Xie, D. G. Mackanic, W. Burke, Z. Bao, Y. Cui, *Mater. Today Nano* **2018**, *4*, 1.
[22] Z. Jiang, Q. Han, S. Wang, H. Wang, *ChemElectroChem* **2019**, *6*, 2970.
[23] S. Xia, X. Wu, Z. Zhang, Y. Cui, W. Liu, *Chem* **2019**, *5*, 753.
[24] A. Gurung, J. Pokharel, A. Baniya, R. Pathak, K. Chen, B. S. Lamsal, N. Ghimire, W. H. Zhang, Y. Zhou, Q. Qiao, *Sustainable Energy Fuels* **2019**, *3*, 3279.
[25] Z. Ding, J. Li, J. Li, C. An, *J. Electrochem. Soc.* **2020**, *167*, 070541.
[26] G. Cui, *Matter* **2020**, *2*, 805.
[27] K. Kerman, A. Luntz, V. Viswanathan, Y.-M. Chiang, Z. Chen, *J. Electrochem. Soc.* **2017**, *164*, A1731.
[28] C. Yu, S. Ganapathy, E. R. H. V. Eck, H. Wang, S. Basak, Z. Li, M. Wagemaker, *Nat. Commun.* **2017**, *8*, 1086.
[29] X. B. Cheng, C. Z. Zhao, Y. X. Yao, H. Liu, Q. Zhang, *Chem* **2019**, *5*, 74.
[30] Y. Hu, X. Sun, *J. Mater. Chem. A* **2014**, *2*, 10712.
[31] Y. S. Jung, D. Y. Oh, Y. J. Nam, K. H. Park, *Isr. J. Chem.* **2015**, *55*, 472.
[32] Z. Gao, H. Sun, L. Fu, F. Ye, Y. Zhang, W. Luo, Y. Huang, *Adv. Mater.* **2018**, *30*, 1705702.
[33] L. Zhou, C. Y. Kwok, A. Shyamsunder, Q. Zhang, X. Wu, L. F. Nazar, *Energy Environ. Sci.* **2020**, *13*, 2056.
[34] C. Huo, Z. Yan, X. Song, H. Zeng, *Sci. Bull.* **2015**, *60*, 1994.
[35] X. Zhang, L. Hou, A. Ciesielski, P. Samorì, *Adv. Energy Mater.* **2016**, *6*, 1600671.
[36] X. Wang, Q. Weng, Y. Yang, Y. Bando, D. Golberg, *Chem. Soc. Rev.* **2016**, *45*, 4042.
[37] B. Li, H. Xu, Y. Ma, S. Yang, *Nanoscale Horiz.* **2019**, *4*, 77.
[38] R. Mas-Ballesté, C. Gómez-Navarro, J. Gómez-Herrero, F. Zamora, *Nanoscale* **2011**, *3*, 20.
[39] T. Zhou, W. Lv, J. Li, G. Zhou, Y. Zhao, S. Fan, B. Liu, B. Li, F. Kang, Q. H. Yang, *Energy Environ. Sci.* **2017**, *10*, 1694.
[40] P. Lu, L. Liu, S. Wang, J. Xu, J. Peng, W. Yan, Q. Wang, H. Li, L. Chen, F. Wu, *Adv. Mater.* **2021**, *33*, 2100921.
[41] L. Shi, T. Zhao, *J. Mater. Chem. A* **2017**, *5*, 3735.
[42] R. Dong, T. Zhang, X. Feng, *Chem. Rev.* **2018**, *118*, 6189.
[43] D. H. Liu, Z. Bai, M. Li, A. Yu, D. Luo, W. Liu, L. Yang, J. Lu, K. Amine, Z. Chen, *Chem. Soc. Rev.* **2020**, *49*, 5407.

© 2022 Wiley-VCH GmbH

15214095, 2022, 16, Downloaded from https://onlinelibrary.wiley.com/doi/10.1002/adma.202108079 by Xian Jiaotong University, Wiley Online Library on [06/06/2024]. See the Terms and Conditions (https://onlinelibrary.wiley.com/terms-and-conditions) on Wiley Online Library for rules of use; OA articles are governed by the applicable Creative Commons License

[44] D. Luo, L. Zheng, Z. Zhang, M. Li, Z. Chen, R. Cui, Y. Shen, G. Li, R. Feng, S. Zhang, G. Jiang, L. Chen, A. Yu, X. Wang, *Nat. Commun.* **2021**, *12*, 186.
[45] F. Zhao, S. H. Alahakoon, K. Adair, S. Zhang, W. Xia, W. Li, C. Yu, R. Feng, Y. Hu, J. Liang, X. Lin, Y. Zhao, X. Yang, T. K. Sham, H. Huang, L. Zhang, S. Zhao, S. Lu, Y. Huang, X. Sun, *Adv. Mater.* **2021**, *33*, 2006577.
[46] B. Ren, G. Wen, L. Ricardez-Sandoval, E. Croiset, *J. Power Sources* **2021**, *490*, 229488.
[47] G. Wen, D. U. Lee, B. Ren, F. M. Hassan, G. Jiang, Z. P. Cano, J. Gostick, E. Croiset, Z. Bai, L. Yang, Z. Chen, *Adv. Energy Mater.* **2018**, *8*, 1802427.
[48] C. Wang, S. Hwang, M. Jiang, J. Liang, Y. Sun, K. Adair, M. Zheng, S. Mukherjee, X. Li, R. Li, H. Huang, S. Zhao, L. Zhang, S. Lu, J. Wang, C. V. Singh, D. Su, X. Sun, *Adv. Energy Mater.* **2021**, *11*, 2100210.
[49] P. Yang, S. Fan, Z. Chen, G. Bao, S. Zuo, C. Qi, *Appl. Catal., B* **2018**, *239*, 114.
[50] N. O. Weiss, H. Zhou, L. Liao, Y. Liu, S. Jiang, Y. Huang, X. Duan, *Adv. Mater.* **2012**, *24*, 5782.
[51] A. Lerf, H. He, M. Forster, J. Klinowski, *J. Phys. Chem. B* **1998**, *102*, 4477.
[52] D. R. Dreyer, S. Murali, Y. Zhu, R. S. Ruoff, C. W. Bielawski, *J. Mater. Chem.* **2011**, *21*, 3443.
[53] P. Kumbhakar, C. Chowde Gowda, P. L. Mahapatra, M. Mukherjee, K. D. Malviya, M. Chaker, A. Chandra, B. Lahiri, P. M. Ajayan, D. Jariwala, A. Singh, C. S. Tiwary, *Mater. Today* **2021**, *45*, 142.
[54] R. Li, Y. Cheng, W. Huang, *Small* **2018**, *14*, 1802091.
[55] Q. Jiang, Y. Lei, H. Liang, K. Xi, C. Xia, H. N. Alshareef, *Energy Storage Mater.* **2020**, *27*, 78.
[56] A. Pakdel, Y. Bando, D. Golberg, *Chem. Soc. Rev.* **2014**, *43*, 934.
[57] P. J. Waller, F. Gándara, O. M. Yaghi, Accounts of Chemical Research 2015, 48 (12), 3053-3063
[58] A. E. Thorarinsdottir, T. D. Harris, *Chem. Rev.* **2020**, *120*, 8716.
[59] S. Wang, L. Yang, G. He, B. Shi, Y. Li, H. Wu, R. Zhang, S. Nunes, Z. Jiang, *Chem. Soc. Rev.* **2020**, *49*, 1071.
[60] G. Kucinskis, G. Bajars, J. Kleperis, *J. Power Sources* **2013**, *240*, 66.
[61] H. Kim, K. Y. Park, J. Hong, K. Kang, *Sci. Rep.* **2014**, *4*, 5278.
[62] S. Wu, R. Ge, M. Lu, R. Xu, Z. Zhang, *Nano Energy* **2015**, *15*, 379.
[63] A. K. Geim, **2009**, *324*, 1530.
[64] R. C. Xu, X. L. Wang, S. Z. Zhang, Y. Xia, X. H. Xia, J. B. Wu, J. P. Tu, *J. Power Sources* **2018**, *374*, 107.
[65] A. T. S. Wee, *ACS Nano* **2012**, *6*, 5739.
[66] D. Wei, S. Haque, P. Andrew, J. Kivioja, T. Ryhänen, A. Pesquera, A. Centeno, B. Alonso, A. Chuvilin, A. Zurutuza, *J. Mater. Chem. A* **2013**, *1*, 3177.
[67] K. S. Novoselov, A. K. Geim, S. V. Morozov, D. Jiang, Y. Zhang, S. V. Dubonos, V. Grigorieva, A. Firsov, *Science* **2004**, *306*, 666.
[68] J. Mei, T. Liao, Z. Sun, *J. Energy Chem.* **2018**, *27*, 117.
[69] V. Augustyn, Y. Gogotsi, *Joule* **2017**, *1*, 443.
[70] V. Augustyn, *J. Mater. Res.* **2017**, *32*, 2.
[71] D. Akinwande, N. Petrone, J. Hone, *Nat. Commun.* **2014**, *5*, https://doi.org/10.1038/ncomms6678.
[72] J. Mannhart, D. G. Schlom, *Science* **2010**, *327*, 1607.
[73] N. Mahmood, I. A. De Castro, K. Pramoda, K. Khoshmanesh, S. K. Bhargava, K. Kalantar-Zadeh, *Energy Storage Mater.* **2019**, *16*, 455.
[74] K. Zhang, M. Park, L. Zhou, G. H. Lee, W. Li, Y. M. Kang, J. Chen, *Adv. Funct. Mater.* **2016**, *26*, 6728.
[75] H. Yuan, L. Kong, T. Li, Q. Zhang, *Chin. Chem. Lett.* **2017**, *28*, 2180.
[76] X. Chen, H. J. Peng, R. Zhang, T. Z. Hou, J. Q. Huang, B. Li, Q. Zhang, *ACS Energy Lett.* **2017**, *2*, 795.
[77] D. W. Murphy, F. A. Trumbore, *J. Cryst. Growth* **1977**, *39*, 185.
[78] X. Huang, Z. Zeng, H. Zhang, *Chem. Soc. Rev.* **2013**, *42*, 1934.
[79] X. Xu, W. Liu, Y. Kim, J. Cho, *Nano Today* **2014**, *9*, 604.
[80] W. Qiu, N. Yang, D. Luo, J. Wang, L. Zheng, Y. Zhu, E. M. Akinoglu, Q. Huang, L. Shui, R. Wang, G. Zhou, X. Wang, Z. Chen, *Appl. Catal., B* **2021**, *293*, 120216.
[81] Z. Liu, Y. Gong, W. Zhou, L. Ma, J. Yu, J. C. Idrobo, J. Jung, A. H. Macdonald, R. Vajtai, J. Lou, P. M. Ajayan, *Nat. Commun.* **2013**, *4*, 2541.
[82] Z. Q. Duan, Y. T. Liu, X. M. Xie, X. Y. Ye, X. D. Zhu, *Chem. – Asian J.* **2016**, *11*, 828.
[83] L. H. Li, J. Cervenka, K. Watanabe, T. Taniguchi, Y. Chen, *ACS Nano* **2014**, *8*, 1457.
[84] J. Xie, L. Liao, Y. Gong, Y. Li, F. Shi, A. Pei, J. Sun, R. Zhang, B. Kong, R. Subbaraman, J. Christensen, Y. Cui, *Sci. Adv.* **2017**, *3*, eaao3170.
[85] V. Guerra, C. Wan, T. McNally, *Prog. Mater. Sci.* **2019**, *100*, 170.
[86] C. R. Dean, A. F. Young, I. Meric, C. Lee, L. Wang, S. Sorgenfrei, K. Watanabe, T. Taniguchi, P. Kim, K. L. Shepard, J. Hone, *Nat. Nanotechnol.* **2010**, *5*, 722.
[87] R. Decker, Y. Wang, V. W. Brar, W. Regan, H. Z. Tsai, Q. Wu, W. Gannett, A. Zettl, M. F. Crommie, *Nano Lett.* **2011**, *11*, 2291.
[88] J. Xue, J. Sanchez-Yamagishi, D. Bulmash, P. Jacquod, A. Deshpande, K. Watanabe, T. Taniguchi, P. Jarillo-Herrero, B. J. Leroy, *Nat. Mater.* **2011**, *10*, 282.
[89] H. Dou, B. Jiang, M. Xu, Z. Zhang, G. Wen, F. Peng, A. Yu, Z. Bai, Y. Sun, L. Zhang, Z. Jiang, Z. Chen, *Angew. Chem.* **2019**, *131*, 14107.
[90] C. Zhao, C. S. Diercks, C. Zhu, N. Hanikel, X. Pei, O. M. Yaghi, *J. Am. Chem. Soc.* **2018**, *140*, 16438.
[91] M. Martínez-Abadiá, C. T. Stoppiello, K. Strutynski, B. Lerma-Berlanga, C. Martí-Gastaldo, A. Saeki, M. Melle-Franco, A. N. Khlobystov, A. Mateo-Alonso, *J. Am. Chem. Soc.* **2019**, *141*, 14403.
[92] S. B. Alahakoon, S. D. Diwakara, C. M. Thompson, R. A. Smaldone, *Chem. Soc. Rev.* **2020**, *49*, 1344.
[93] J. Liu, P. Lyu, Y. Zhang, P. Nachtigall, Y. Xu, *Adv. Mater.* **2018**, *30*, 1705401.
[94] L. Yang, H. Yang, H. Wu, L. Zhang, H. Ma, Y. Liu, Y. Wu, Y. Ren, X. Wu, Z. Jiang, *J. Mater. Chem. A* **2021**, *9*, 12636.
[95] W. Zheng, C. S. Tsang, L. Y. S. Lee, K. Y. Wong, *Mater. Today Chem.* **2019**, *12*, 34.
[96] J. Park, M. Lee, D. Feng, Z. Huang, A. C. Hinckley, A. Yakovenko, X. Zou, Y. Cui, Z. Bao, *J. Am. Chem. Soc.* **2018**, *140*, 10315.
[97] M. L. Aubrey, J. R. Long, *J. Am. Chem. Soc.* **2015**, *137*, 13594.
[98] D. Sheberla, J. C. Bachman, J. S. Elias, C. J. Sun, Y. Shao-Horn, M. Dincă, *Nat. Mater.* **2017**, *16*, 220.
[99] W. Qiu, X. Y. Xie, J. Qiu, W. H. Fang, R. Liang, X. Ren, X. Ji, G. Cui, A. M. Asiri, G. Cui, B. Tang, X. Sun, *Nat. Commun.* **2018**, *9*, 3485.
[100] Z. Lin, A. McCreary, N. Briggs, S. Subramanian, K. Zhang, Y. Sun, X. Li, N. J. Borys, H. Yuan, S. K. Fullerton-Shirey, A. Chernikov, H. Zhao, S. McDonnell, A. M. Lindenberg, K. Xiao, B. J. Le Roy, M. Drndić, J. C. M. Hwang, J. Park, M. Chhowalla, R. E. Schaak, A. Javey, M. C. Hersam, J. Robinson, M. Terrones, *2D Mater.* **2016**, *3*, 042001.
[101] N. Briggs, B. Bersch, Y. Wang, J. Jiang, R. J. Koch, N. Nayir, K. Wang, M. Kolmer, W. Ko, A. De La, F. Duran, S. Subramanian, C. Dong, J. Shallenberger, M. Fu, Q. Zou, Y. Chuang, Z. Gai, A. Li, A. Bostwick, C. Jozwiak, C. Chang, E. Rotenberg, J. Zhu, *Nat. Mater.* **2020**, *19*, 637.
[102] E. Gao, S. Z. Lin, Z. Qin, M. J. Buehler, X. Q. Feng, Z. Xu, *J. Mech. Phys. Solids* **2018**, *115*, 248.
[103] V. Nicolosi, M. Chhowalla, M. G. Kanatzidis, M. S. Strano, J. N. Coleman, *Science* **2013**, *340*, 72.
[104] J. Lu, Z. Chen, F. Pan, L. A. Curtiss, K. Amine, *Nat. Nanotechnol.* **2010**, *11*, 1031.
[105] E. Gao, Z. Xu, *J. Appl. Mech.* **2015**, *82*, 121012.
[106] X. Cai, Y. Luo, B. Liu, H. M. Cheng, *Chem. Soc. Rev.* **2018**, *47*, 6224.

© 2022 Wiley-VCH GmbH

15214095, 2022, 16, Downloaded from https://onlinelibrary.wiley.com/doi/10.1002/adma.202108079 by Xian Jiaotong University, Wiley Online Library on [06/06/2024]. See the Terms and Conditions (https://onlinelibrary.wiley.com/terms-and-conditions) on Wiley Online Library for rules of use; OA articles are governed by the applicable Creative Commons License

[107] J. Y. Moon, M. Kim, S. Il Kim, S. Xu, J. H. Choi, D. Whang, K. Watanabe, T. Taniguchi, D. S. Park, J. Seo, S. H. Cho, S. K. Son, J. H. Lee, *Sci. Adv.* **2020**, *6*, eabc6601.
[108] J. N. Coleman, M. Lotya, A. O'Neill, S. D. Bergin, P. J. King, U. Khan, K. Young, A. Gaucher, S. De, R. J. Smith, I. V. Shvets, S. K. Arora, G. Stanton, H. Y. Kim, K. Lee, G. T. Kim, G. S. Duesberg, T. Hallam, J. J. Boland, J. J. Wang, J. F. Donegan, J. C. Grunlan, G. Moriarty, A. Shmeliov, R. J. Nicholls, J. M. Perkins, E. M. Grieveson, K. Theuwissen, D. W. McComb, P. D. Nellist, *et al.*, *Science* **2011**, *331*, 568.
[109] H. Chen, X. Feng, Y. Huang, Y. Huang, J. A. Rogers, *J. Mech. Phys. Solids* **2013**, *61*, 1737.
[110] H. Chen, S. Chen, *J. Phys. D: Appl. Phys.* **2013**, *46*, 435305.
[111] J. Yu, J. Li, W. Zhang, H. Chang, *Chem. Sci.* **2015**, *6*, 6705.
[112] T. Gao, S. Xie, Y. Gao, M. Liu, Y. Chen, Y. Zhang, Z. Liu, *ACS Nano* **2011**, *5*, 9194.
[113] K. Yan, H. Peng, Y. Zhou, H. Li, Z. Liu, *Nano Lett.* **2011**, *11*, 1106.
[114] M. Wang, S. K. Jang, W. J. Jang, M. Kim, S. Y. Park, S. W. Kim, S. J. Kahng, J. Y. Choi, R. S. Ruoff, Y. J. Song, S. Lee, *Adv. Mater.* **2013**, *25*, 2746.
[115] C. M. Seah, S. P. Chai, A. R. Mohamed, *Carbon* **2014**, *70*, 1.
[116] L. Li, Y. Yu, G. J. Ye, Q. Ge, X. Ou, H. Wu, D. Feng, X. H. Chen, Y. Zhang, *Nat. Nanotechnol.* **2014**, *9*, 372.
[117] A. B. Bourlinos, V. Georgakilas, R. Zboril, T. A. Sterioti, A. K. Stubos, *Small* **2009**, *5*, 1841.
[118] Y. Yu, C. Li, Y. Liu, L. Su, Y. Zhang, L. Cao, *Sci. Rep.* **2013**, *3*, 1866.
[119] S. Witomska, T. Leydecker, A. Ciesielski, P. Samorì, *Adv. Funct. Mater.* **2019**, *29*, 1901126.
[120] G. H. Park, K. Nielsch, A. Thomas, *Adv. Mater. Interfaces* **2019**, *6*, 1800688.
[121] Y. Zhang, T. Zuo, J. Popovic, K. Lim, Y. Yin, *Mater. Today* **2020**, *33*, 56.
[122] Y. Wang, B. Liu, Q. Li, S. Cartmell, S. Ferrara, Z. D. Deng, J. Xiao, *J. Power Sources* **2015**, *286*, 330.
[123] J. Lin, Y. Wu, R. Bi, H. Guo, *Sens. Actuators, A* **2017**, *253*, 218.
[124] S. Huang, H. Yang, J. Hu, Y. Liu, K. Wang, H. Peng, H. Zhang, L. Z. Fan, *Small* **2019**, *15*, 32.
[125] J. Wen, Y. Huang, J. Duan, Y. Wu, W. Luo, L. Zhou, C. Hu, L. Huang, X. Zheng, W. Yang, Z. Wen, Y. Huang, *ACS Nano* **2019**, *13*, 14549.
[126] Q. Cheng, A. Li, N. Li, S. Li, A. Zangiabadi, T. De Li, W. Huang, A. C. Li, T. Jin, Q. Song, W. Xu, N. Ni, H. Zhai, M. Dontigny, K. Zaghib, X. Chuan, D. Su, K. Yan, Y. Yang, *Joule* **2019**, *3*, 1510.
[127] A. Kızılaslan, T. Çetinkaya, H. Akbulut, *Adv. Mater. Interfaces* **2020**, *7*, 2001020.
[128] Y. Xue, G. Ma, X. Wang, M. Jin, E. M. Akinoglu, D. Luo, L. Shui, *ACS Appl. Mater. Interfaces* **2021**, *13*, 7334.
[129] S. Lou, F. Zhang, C. Fu, M. Chen, Y. Ma, G. Yin, J. Wang, *Adv. Mater.* **2020**, *33*, 2000721.
[130] Y. Li, Y. Li, Y. Yang, Z. Cui, J. Wang, T. Zhang, *Chem. Commun.* **2020**, *56*, 1725.
[131] L. Cai, H. Wan, Q. Zhang, J. P. Mwizerwa, X. Xu, X. Yao, *ACS Appl. Mater. Interfaces* **2020**, *12*, 33810.
[132] H. Wan, L. Cai, F. Han, J. P. Mwizerwa, C. Wang, X. Yao, *Small* **2019**, *15*, 1905849.
[133] H. Wan, G. Peng, X. Yao, J. Yang, P. Cui, X. Xu, *Energy Storage Mater.* **2016**, *4*, 59.
[134] C. Zhang, Y. Lin, Y. Zhu, Z. Zhang, J. Liu, *RSC Adv.* **2017**, *7*, 19231.
[135] Z. Zhuang, L. Yang, B. Ju, A. Yin, G. Lei, Q. Zhou, Y. Tang, Z. Deng, F. Tu, S. Qin, *Energy Storage* **2020**, *2*, e109.
[136] R. Cao, W. Xu, D. Lv, J. Xiao, J. G. Zhang, *Adv. Energy Mater.* **2015**, *5*, 1402273.
[137] X. Yao, N. Huang, F. Han, Q. Zhang, H. Wan, J. P. Mwizerwa, C. Wang, X. Xu, *Adv. Energy Mater.* **2017**, *7*, 1602923.
[138] Y. Zhang, J. Lai, Y. Gong, Y. Hu, J. Liu, C. Sun, Z. L. Wang, *ACS Appl. Mater. Interfaces* **2016**, *8*, 34309.
[139] Q. Zhang, H. Wan, G. Liu, Z. Ding, J. P. Mwizerwa, X. Yao, *Nano Energy* **2019**, *57*, 771.
[140] Q. Zhang, Z. Ding, G. Liu, H. Wan, J. P. Mwizerwa, J. Wu, X. Yao, *Energy Storage Mater.* **2019**, *23*, 168.
[141] R. C. Xu, X. H. Xia, X. L. Wang, Y. Xia, J. P. Tu, *J. Mater. Chem. A* **2017**, *5*, 2829.
[142] A. L. Santhosha, P. K. Nayak, K. Pollok, F. Langenhorst, P. Adelhelm, *J. Phys. Chem. C* **2019**, *123*, 12126.
[143] Q. Zhang, X. Yao, J. P. Mwizerwa, N. Huang, H. Wan, Z. Huang, X. Xu, *Solid State Ionics* **2018**, *318*, 60.
[144] C. Xing, D. Zhang, K. Cao, S. Zhao, X. Wang, H. Qin, J. Liu, Y. Jiang, L. Meng, *J. Mater. Chem. A* **2015**, *3*, 8742.
[145] N. Kamaya, K. Homma, Y. Yamakawa, M. Hirayama, R. Kanno, M. Yonemura, T. Kamiyama, Y. Kato, S. Hama, K. Kawamoto, A. Mitsui, *Nat. Mater.* **2011**, *10*, 682.
[146] L. Cai, Q. Zhang, J. P. Mwizerwa, H. Wan, X. Yang, X. Xu, X. Yao, *ACS Appl. Mater. Interfaces* **2018**, *10*, 10053.
[147] W. Fang, H. Zhao, Y. Xie, J. Fang, J. Xu, Z. Chen, *ACS Appl. Mater. Interfaces* **2015**, *7*, 13044.
[148] S. Xu, C. Y. Kwok, L. Zhou, Z. Zhang, I. Kochetkov, L. F. Nazar, *Adv. Funct. Mater.* **2021**, *31*, 2004239.
[149] Y. Fujii, D. Ramirez, N. C. Rosero-Navarro, D. Jullian, A. Miura, F. Jaramillo, K. Tadanaga, *ACS Appl. Energy Mater.* **2019**, *2*, 6569.
[150] J. Shi, G. Liu, W. Weng, L. Cai, Q. Zhang, J. Wu, X. Xu, X. Yao, *ACS Appl. Mater. Interfaces* **2020**, *12*, 14079.
[151] Q. Xia, Q. Zhang, S. Sun, F. Hussain, C. Zhang, X. Zhu, F. Meng, K. Liu, H. Geng, J. Xu, F. Zan, P. Wang, L. Gu, H. Xia, *Adv. Mater.* **2021**, *33*, 2003524.
[152] L. Su, L. Liu, J. Hei, H. Chen, L. Wang, Y. Wang, M. Ren, *Part. Part. Syst. Charact.* **2020**, *37*, 2000164.
[153] Q. Zhang, J. P. Mwizerwa, H. Wan, L. Cai, X. Xu, X. Yao, *J. Mater. Chem. A* **2017**, *5*, 23919.
[154] H. Dou, M. Xu, B. Wang, Z. Zhang, G. Wen, Y. Zheng, D. Luo, L. Zhao, A. Yu, L. Zhang, Z. Jiang, Z. Chen, *Chem. Soc. Rev.* **2021**, *50*, 986.
[155] Q. Han, S. Wang, Z. Jiang, X. Hu, H. Wang, *ACS Appl. Mater. Interfaces* **2020**, *12*, 20514.
[156] P. Zhai, N. Peng, Z. Sun, W. Wu, W. Kou, G. Cui, K. Zhao, J. Wang, *J. Mater. Chem. A* **2020**, *8*, 23344.
[157] B. Wang, M. Tang, Y. Wu, Y. Chen, C. Jiang, S. Zhuo, S. Zhu, C. Wang, *ACS Appl. Energy Mater.* **2019**, *2*, 5909.
[158] Y. Li, Z. Sun, D. Liu, Y. Gao, Y. Wang, H. Bu, M. Li, Y. Zhang, G. Gao, S. Ding, *J. Mater. Chem. A* **2020**, *8*, 2021.
[159] S. Gomari, M. Esfandeh, I. Ghasemi, *Solid State Ionics* **2017**, *303*, 37.
[160] A. Dey, S. Karan, S. K. De, *J. Phys. Chem. Solids* **2010**, *71*, 329.
[161] Z. Zhang, R. G. Antonio, K. L. Choy, *J. Power Sources* **2019**, *435*, 226736.
[162] X. Yin, L. Wang, Y. Kim, N. Ding, J. Kong, D. Safanama, Y. Zheng, J. Xu, D. V. M. Repaka, K. Hippalgaonkar, S. W. Lee, S. Adams, G. W. Zheng, *Adv. Sci.* **2020**, *7*, 2001303.
[163] W. Tang, S. Tang, C. Zhang, Q. Ma, Q. Xiang, Y. W. Yang, J. Luo, *Adv. Energy Mater.* **2018**, *8*, 1800866.
[164] W. Tang, S. Tang, X. Guan, X. Zhang, Q. Xiang, J. Luo, *Adv. Funct. Mater.* **2019**, *29*, 1900648.
[165] G. Zheng, S. W. Lee, Z. Liang, H. W. Lee, K. Yan, H. Yao, H. Wang, W. Li, S. Chu, Y. Cui, *Nat. Nanotechnol.* **2014**, *9*, 618.
[166] L.-Y. Yang, D.-X. Wei, M. Xu, Y.-F. Yao, Q. Chen, *Angew. Chem.* **2014**, *126*, 3705.
[167] X. Chen, X. R. Chen, T. Z. Hou, B. Q. Li, X. B. Cheng, R. Zhang, Q. Zhang, *Sci. Adv.* **2019**, *5*, eaau7728.
[168] Y. Li, L. Zhang, Z. Sun, G. Gao, S. Lu, M. Zhu, Y. Zhang, Z. Jia, C. Xiao, H. Bu, K. Xi, S. Ding, *J. Mater. Chem. A* **2020**, *8*, 9579.

© 2022 Wiley-VCH GmbH

15214095, 2022, 16, Downloaded from https://onlinelibrary.wiley.com/doi/10.1002/adma.202108079 by Xian Jiaotong University, Wiley Online Library on [06/06/2024]. See the Terms and Conditions (https://onlinelibrary.wiley.com/terms-and-conditions) on Wiley Online Library for rules of use; OA articles are governed by the applicable Creative Commons License

[169] Z. Sun, Y. Li, S. Zhang, L. Shi, H. Wu, H. Bu, S. Ding, *J. Mater. Chem. A* **2019**, *7*, 11069.
[170] W. Jia, Z. Li, Z. Wu, L. Wang, B. Wu, Y. Wang, Y. Cao, J. Li, *Solid State Ionics* **2018**, *315*, 7.
[171] X. Xu, L. Wang, H. Fei, L. Ci, *J. Mater. Sci. Mater. Electron.* **2019**, *30*, 19119.
[172] P. Geng, S. Zheng, H. Tang, R. Zhu, L. Zhang, S. Cao, H. Xue, H. Pang, *Adv. Energy Mater.* **2018**, *8*, 1703259.
[173] D. Y. Oh, Y. E. Choi, D. H. Kim, Y. G. Lee, B. S. Kim, J. Park, H. Sohn, Y. S. Jung, *J. Mater. Chem. A* **2016**, *4*, 10329.
[174] J. Wu, X. Li, Y. Zhao, L. Liu, W. Qu, R. Luo, R. Chen, Y. Li, Q. Chen, *J. Mater. Chem. A* **2018**, *6*, 20896.
[175] Z. Li, Z. W. Liu, Z. Li, T. X. Wang, F. Zhao, X. Ding, W. Feng, B. H. Han, *Adv. Funct. Mater.* **2020**, *30*, 1909267.
[176] Z. Li, Z. W. Liu, Z. J. Mu, C. Cao, Z. Li, T. X. Wang, Y. Li, X. Ding, B. H. Han, W. Feng, *Mater. Chem. Front.* **2020**, *4*, 1164.
[177] G. Zhang, Y. L. Hong, Y. Nishiyama, S. Bai, S. Kitagawa, S. Horike, *J. Am. Chem. Soc.* **2019**, *141*, 1227.
[178] X. Li, Q. Hou, W. Huang, H. Sen Xu, X. Wang, W. Yu, R. Li, K. Zhang, L. Wang, Z. Chen, K. Xie, K. P. Loh, *ACS Energy Lett.* **2020**, *5*, 3498.
[179] W. Sun, J. Zhang, M. Xie, D. Lu, Z. Zhao, Y. Li, Z. Cheng, S. Zhang, H. Chen, *Nano Lett.* **2020**, *20*, 8120.
[180] Y. Cheng, L. Zhang, Q. Zhang, J. Li, Y. Tang, C. Delmas, T. Zhu, M. Winter, M. S. Wang, J. Huang, *Mater. Today* **2021**, *42*, 137.
[181] Y. Xiang, G. Zheng, Z. Liang, Y. Jin, X. Liu, S. Chen, K. Zhou, J. Zhu, M. Lin, H. He, J. Wan, S. Yu, G. Zhong, R. Fu, Y. Li, Y. Yang, *Nat. Nanotechnol.* **2020**, *15*, 883.
[182] N. Minafra, S. P. Culver, C. Li, A. Senyshyn, W. G. Zeier, *Chem. Mater.* **2019**, *31*, 3794.
[183] B. K. Seidlhofer, B. Jerliu, M. Trapp, E. Hüger, S. Risse, R. Cubitt, H. Schmidt, R. Steitz, M. Ballauff, *ACS Nano* **2016**, *10*, 7458.
[184] I. Robinson, R. Harder, *Nat. Mater.* **2009**, *8*, 291.
[185] Y. Deng, C. Eames, J. N. Chotard, F. Lalèire, V. Seznec, S. Emge, O. Pecher, C. P. Grey, C. Masquelier, M. S. Islam, *J. Am. Chem. Soc.* **2015**, *137*, 9136.
[186] R. Kun, F. Langer, M. Delle Piane, S. Ohno, W. G. Zeier, M. Gockeln, L. Colombi Ciacchi, M. Busse, I. Fekete, *ACS Appl. Mater. Interfaces* **2018**, *10*, 37188.
[187] G. Vardar, W. J. Bowman, Q. Lu, J. Wang, R. J. Chater, A. Aguadero, R. Seibert, J. Terry, A. Hunt, I. Waluyo, D. D. Fong, A. Jarry, E. J. Crumlin, S. L. Hellstrom, Y. Chiang, B. Yildiz, *Chem. Mater.* **2018**, *30*, 6259.
[188] M. B. Dixit, J.-S. Park, P. Kenesei, J. Almer, K. B. Hatzell, *Energy Environ. Sci.* **2021**, *14*, 4672.
[189] C. Wu, F. Feng, Y. Xie, *Chem. Soc. Rev.* **2013**, *42*, 5157.
[190] J. Wang, Y. C. K. Chen-Wiegart, C. Eng, Q. Shen, J. Wang, *Nat. Commun.* **2016**, *7*, 12372.
[191] W. Li, J. Liang, M. Li, K. R. Adair, X. Li, Y. Hu, Q. Xiao, R. Feng, R. Li, L. Zhang, S. Lu, H. Huang, S. Zhao, T. K. Sham, X. Sun, *Chem. Mater.* **2020**, *32*, 7019.
[192] F. Shen, M. B. Dixit, X. Xiao, K. B. Hatzell, *ACS Energy Lett.* **2018**, *3*, 1056.
[193] C. Dietrich, R. Koerver, M. W. Gaultois, G. Kieslich, G. Cibin, J. Janek, W. G. Zeier, *Phys. Chem. Chem. Phys.* **2018**, *20*, 20088.
[194] Y. Nomura, K. Yamamoto, T. Hirayama, M. Ohkawa, E. Igaki, N. Hojo, K. Saitoh, *Nano Lett.* **2018**, *18*, 5892.
[195] T. Liu, L. Lin, X. Bi, L. Tian, K. Yang, J. Liu, M. Li, Z. Chen, J. Lu, K. Amine, K. Xu, F. Pan, *Nat. Nanotechnol.* **2019**, *14*, 50.
[196] F. Sagane, R. Shimokawa, H. Sano, H. Sakaebe, Y. Iriyama, *J. Power Sources* **2013**, *225*, 245.
[197] K. E. Madsen, K. L. Bassett, K. Ta, B. A. Sforzo, K. E. Matusik, A. L. Kastengren, A. A. Gewirth, *Adv. Mater. Interfaces* **2020**, *7*, 2000751.

Qianyi Ma is a MASc student from the department of chemical engineering at University of Waterloo, Canada. He received his bachelor's degree in University of Waterloo/Beijing Jiaotong University in 2020. His research interests are electrochemical energy storage and conversion, especially for the research of composite solid-state electrolyte for lithium metal battery, electrolyte design in aqueous Zn-ions battery at extreme-low temperature.

Yun Zheng is a post-doctoral fellow from the department of chemical engineering at University of Waterloo, Canada. He received his Ph.D. in chemical engineering from Tsinghua University in 2019, His research interests are electrochemical energy storage and conversion, especially for the research of composite solid-state electrolyte for lithium metal battery, high temperature electrolysis of CO_2/H_2O to produce sustainable fuels using solid oxide electrolysis cells, as well as the heterostructured electrode materials for solid oxide fuel cells.

© 2022 Wiley-VCH GmbH

15214095, 2022, 16, Downloaded from https://onlinelibrary.wiley.com/doi/10.1002/adma.202108079 by Xian Jiaotong University, Wiley Online Library on [06/06/2024]. See the Terms and Conditions (https://onlinelibrary.wiley.com/terms-and-conditions) on Wiley Online Library for rules of use; OA articles are governed by the applicable Creative Commons License

Dan Luo received his Ph.D. degree in chemical engineering from University of Waterloo and now he is an associate researcher of Advanced Optoelectronics & School of Information and Optoelectronic Science and Engineering, South China Normal University. He has published over 80 papers with a H-index of 30. His research is currently focused on the development of novel electrode materials and electrolyte design for rechargeable lithium–sulfur batteries and lithium metal batteries.

Xin Wang received his Ph.D. degree from Beijing Normal University. He is currently a professor at South China Normal University. His research interests focus on the development of advanced materials and their applications in photocatalysis, energy storage devices, and lithium metal batteries.

Zhongwei Chen received his Ph.D. degree from University of California, Riverside. He is Canada research chair professor (Tier 1) in advanced materials for clean energy at the University of Waterloo, fellow of Royal Society of Canada, fellow of the Canadian Academy of Engineering, and the vice president of the International Academy of Electrochemical Energy Science (IAOEES). He has published over 400 papers with a H-index of 98. His research interests focus on the development of advanced materials and electrodes for electrochemical energy storage, electrocatalysis, and lithium metal batteries.

© 2022 Wiley-VCH GmbH

15214095, 2022, 16, Downloaded from https://onlinelibrary.wiley.com/doi/10.1002/adma.202108079 by Xian Jiaotong University, Wiley Online Library on [06/06/2024]. See the Terms and Conditions (https://onlinelibrary.wiley.com/terms-and-conditions) on Wiley Online Library for rules of use; OA articles are governed by the applicable Creative Commons License